Functional significance of the taper of vertebrate cone photoreceptors

Ferenc I. Hárosi[1] and Iñigo Novales Flamarique[2]

[1]Laboratory of Sensory Physiology, Marine Biological Laboratory, Woods Hole, MA 02543
[2]Department of Biological Sciences, Simon Fraser University, Burnaby, British Columbia V3J 4M5, Canada

Vertebrate photoreceptors are commonly distinguished based on the shape of their outer segments: those of cones taper, whereas the ones from rods do not. The functional advantages of cone taper, a common occurrence in vertebrate retinas, remain elusive. In this study, we investigate this topic using theoretical analyses aimed at revealing structure–function relationships in photoreceptors. Geometrical optics combined with spectrophotometric and morphological data are used to support the analyses and to test predictions. Three functions are considered for correlations between taper and functionality. The first function proposes that outer segment taper serves to compensate for self-screening of the visual pigment contained within. The second function links outer segment taper to compensation for a signal-to-noise ratio decline along the longitudinal dimension. Both functions are supported by the data: real cones taper more than required for these compensatory roles. The third function relates outer segment taper to the optical properties of the inner compartment whereby the primary determinant is the inner segment's ability to concentrate light via its ellipsoid. In support of this idea, the rod/cone ratios of primarily diurnal animals are predicted based on a principle of equal light flux gathering between photoreceptors. In addition, ellipsoid concentration factor, a measure of ellipsoid ability to concentrate light onto the outer segment, correlates positively with outer segment taper expressed as a ratio of characteristic lengths, where critical taper is the yardstick. Depending on a light-funneling property and the presence of focusing organelles such as oil droplets, cone outer segments can be reduced in size to various degrees. We conclude that outer segment taper is but one component of a miniaturization process that reduces metabolic costs while improving signal detection. Compromise solutions in the various retinas and retinal regions occur between ellipsoid size and acuity, on the one hand, and faster response time and reduced light sensitivity, on the other.

The Journal of General Physiology

INTRODUCTION

Since the early days of vision research, pioneered by the work of Hannover (1840), Müller (1856), and Schultze (1866, 1867), vertebrate photoreceptors have been classified as rods and cones by morphological criteria. Schultze (1866) correlated the visual habits of animals with the relative preponderance of rods and cones in their retinas; this led him to formulate the concept upon which the Duplicity Theory rests. The premise of this theory is that cones are the receptors for photopic (bright light) vision, whereas rods are the receptors for scotopic (dim light) sensing. Schultze (1866, 1867) arrived at the correct conclusion that cones mediate color perception.

Subsequent to Schultze's time, visual cells have been described with intermediate morphological, physiological, and molecular attributes that tend to blur the distinction between rods and cones (Walls, 1963; Pedler, 1965; Crescitelli, 1972; Kojima et al., 1992; Ma et al., 2001; Collin et al., 2004; Zhang et al., 2006). Nevertheless, the old classification has endured as regards to the vertebrate retina: its photoreceptors are rods and cones wherein cones typically exhibit a tapered outer segment, whereas rods do not. The functional significance of this distinguishing feature, so prevalent in nature, remains largely unexplored.

One of the potential benefits of tapering cone outer segments was introduced by Hodgkin and O'Bryan (1977) with their concept of critical taper. In their study of turtle cone electrical responses, these authors considered two limiting cases of cone geometry: the cylindrical (untapered) form and another, in which the "outer segment tapers in such a way that all molecules have an equal chance of absorbing a quantum" (Hodgkin and O'Bryan, 1977). In the latter case, the outer segment must taper at a specific, critical angle, and light must be funneled by complete internal reflection from the broad to the narrow end of cone outer segments (Hodgkin and O'Bryan, 1977). The significance of critical taper is as follows.

Rods and cones are highly specialized cells with unusual properties. First, the sensory visual pigments that they use are extremely absorbent; i.e., they possess very high extinction coefficients, corresponding to large molecular absorption cross sections (Hárosi and MacNichol, 1974). Second, visual pigment molecules are densely

Dr. Hárosi died in November 2008.
Correspondence to Iñigo Novales Flamarique: inigo@sfu.ca

The Rockefeller University Press $30.00
J. Gen. Physiol. Vol. 139 No. 2 159–187
www.jgp.org/cgi/doi/10.1085/jgp.201110692

packed in lamellar membranes, which, in turn, are tightly stacked in hundreds of layers within the outer segment (the molecular packing within the membrane and the tightness of lamellar packing are probably as high as functional constraints will allow; see Wen et al., 2009). Consequently, the pigment-laden lamellae in the more proximal layers act as light filters for the more distal layers. This phenomenon is known as self-screening (Brindley, 1970). As a result of self-screening, light quanta arriving in the physiological setting have a greater probability of being absorbed near the base of an outer segment than toward the apex. Thus, in a cylindrical rod, where lamellae are of equal size, signal generation declines steadily in more distal layers with a concomitant decline in efficiency (i.e., photocurrent production per unit volume; Schnapf, 1983). One possible way to improve performance is to trim the volume slices along the length of outer segments in proportion to the fall-off of lamellar absorption caused by self-screening. A conical structure could accomplish this. Tapering is considered critical when the trimming of lamellar cross section along the taper is exactly proportional to the fall-off of absorption rate, resulting in uniform efficiency (Hodgkin and O'Bryan, 1977). This idea, which was neither generalized nor experimentally tested, is the basis for the first potential function, overcoming signal loss caused by self-screening, that we evaluate in this study.

A second function considered is that outer segments taper to enhance the signal-to-noise ratio along their lengths. Accordingly, taper would also be driven by another outer segment function: signal generation. Although the generation of signal and associated noise in photoreceptors are complex phenomena, in part because of the stochastic nature of underlying processes, such as the opening and closing of ionic channels or the binding and release of ligands at receptor sites in the enzymatic cascade of the light response, there is a consensus on the existence of thermal activation of visual pigment molecules and cGMP phosphodiesterases, both components giving rise to noise (Rieke and Baylor, 1996, 2000; Holcman and Korenbrot, 2005). Based on current understanding, the receptor signal consists of a photocurrent generated through a narrow circumferential region of the outer segment membrane in response to the number of quanta absorbed in the adjacent volume containing one or a few lamellae (Baylor, 1987). Noise, on the other hand, is assumed, on the most basic level, to be proportional to the total number of visual pigment molecules or cGMP phosphodiesterases contained in the same volume (Rieke and Baylor 1996, 2000; Sampath and Baylor, 2002; Holcman and Korenbrot, 2005). Either way, the signal-to-noise ratio is expected to diminish along the outer segment length (z direction) in cylindrical cells. With a tapered outer segment, however, consecutive lamellae are progressively reduced in cross section, leading to diminution of noise along the way.

The third and last function that we evaluate, efficient light collection and utilization of biomaterials, is based on the hypothesis that outer segment taper follows the optical properties of the inner segment. Rather than considering outer segment taper to be tied up with strictly outer segment functions, this idea proposes a multifaceted interdependence between inner and outer segments, as suggested by morphology.

Both cones and rods feature three distinct compartments or subcellular organelles: an outer segment (limb), specialized for trapping light; an inner segment (cone ellipsoid), concerned primarily with energy production and homeostatic functions; and a synaptic apparatus that communicates with other neurons (Fein and Szuts, 1982). Cone ellipsoids are usually the most conspicuous of the photoreceptor compartments in practically every retina, with primate foveal cones being a notable exception (Borwein et al., 1980; Packer et al., 1989; Hoang et al., 2002). Cones are always broadest at their ellipsoid and tend to taper toward the outer segment, to which they attach closely (Fein and Szuts, 1982). In some fish retinas, the two cone compartments appear as one confluent unit, so that it is hard to discern through the light microscope where the ellipsoid ends and the base of the outer segment begins. In contrast, rods rarely have any difference in width between the two limbs. Shape and size variation notwithstanding, it is always the inner segment wherefrom light enters the outer segment in the physiological setting. For these reasons, it seems logical to consider the two compartments combined as one optical unit.

Cone ellipsoids tend to taper from the thickest proximal region toward the distal outer limb, and this, most likely, is a ploy to concentrate light (Winston 1970, 1981). And if that is so, the outer segment taper may be dependent on the light-gathering property of the inner segment. This idea is also bolstered by the observation that cones with oil droplets tend to have more tapered outer segments than those without this organelle (Nilsson, 1965; Kolb and Jones, 1982; Röhlich and Szél, 2000; Bailes et al., 2006). In view of the high refractive index values of oil droplets (Ives et al., 1983), there is no doubt about their refractive role (Baylor and Fettiplace, 1975; Young and Martin, 1984). Given some light concentration property, cone ellipsoids could funnel parallel incident light into converging (conical) beams, which, when projected onto smaller lamellar areas, could result in equal photon catch (and signal) maintained at reduced noise. Even in the presence of light losses, increased tapering should be advantageous for the gains to be made in improved signal to noise (by lamellar shrinkage) and in savings in detector material (by volume reduction). A practical solution ought to balance the advantages against the concomitant drawbacks, such as

reduced acuity and some light loss by ellipsoid leakage. As such, a standard cone should not exist, but there should be variously tapered structures in nature that represent compromise solutions to different sets of constraints. Although the third function does not lend itself to testing via a single mathematical relationship, its validity can be ascertained by examining structure–function relationships in different species and comparing outer and inner segment taper-related variables that, from the aforementioned reasoning, should be positively correlated.

Our analysis of cone taper focuses on photoreceptor properties that have been routinely selected for during the course of evolution such as improved signal detection and metabolic savings by efficient use of biomaterials (see, for instance, the photoreceptor innovations of anchovies; Novales Flamarique, 2011). Early vertebrates, like extant hagfishes and larval ascidians, evolved ciliary photoreceptors that acted as shadow detectors, presumably conferring some of these animals an advantage in dim light environments (Collin, 2010). Natural selection acting on mutations to these ancestral designs led to a large number of novel photoreceptor features, including changes in outer segment shape (from conical to rodlike and vice versa, the transmutation hypothesis; Walls, 1963), multiple photopigments for color vision (Bowmaker, 2008), phototransduction enzymes with varying response kinetics (Hisatomi and Tokunaga, 2002), and, with a focusing eye, photoreceptor mosaics that improved overall sensitivity and/or visual acuity (van der Meer, 1992). As per other selective traits, the shape and size of photoreceptors are expected to vary, and each form may subserve multiple functions, though perhaps none optimally. Indeed, natural selection may retain a given form because it is either nondeleterious or because it confers some advantage to the individual (Bell, 2009). We therefore surmised that our analysis could reveal various advantages of taper to cone photoreceptor function.

The primary thrust of this study is theoretical. Attention is focused on morphological and biochemical properties of vertebrate photoreceptors. The aim is to gain insight into the principles governing their structure and function. In addition to the analytical approach, experimental results are used for testing theoretical predictions. The empirical data include cellular dimensions, which were derived by light and electron microscopic measurements, in situ visual pigment determinations by microspectrophotometry, in vitro visual pigment data obtained by spectrophotometry, electrophysiological determinations, and comparative anatomy. The cited empirical data are derived from either published articles in the literature or hitherto unpublished work from our laboratories. The three potential functions of cone taper that we evaluate are considered in sequence; for each, the consequences and ramifications are examined.

MATERIALS AND METHODS

Animals

The majority of data in this study originated from animals used in published works, either our own or those of others. However, some measurements were taken from studies that have yet to appear in the literature. These measurements originated from goldfish (*Carassius auratus*), common carp (*Cyprinus carpio*), zebrafish (*Danio rerio*), three-spine stickleback (*Gasterosteus acuelatus*), blue gill sunfish (*Lepomis macrochirus*), green sunfish (*Lepomis cyanellus*), rainbow trout (*Oncorhynchus mykiss*), coho salmon (*Oncorhynchus kisutch*), chinook salmon (*Oncorhynchus tschawytscha*), African clawed frog (*Xenopus laevis*), northern leopard frog (*Rana pipiens*), American bullfrog (*Rana catesbeiana*), Canada goose (*Branta canadensis*), green-winged teal (*Anas crecca carolinensis*), red-eared slider turtle (*Trachemys scripta elegans*), and mouse (*Mus musculus*). Animals were obtained from the following locations: zebrafish, local pet shop supplier in Burnaby (British Columbia, Canada); three-spine stickleback, Swan Lake (Victoria, British Columbia, Canada); blue gill sunfish, ponds around the Woods Hole, MA area; rainbow trout, Lower Mainland Trout Hatchery (Abbotsford, British Columbia, Canada); coho salmon and chinook salmon; Capilano River hatchery (North Vancouver, British Columbia, Canada); common carp, green sunfish, African clawed frogs, and northern leopard frogs, Marine Resources Centre of the Marine Biological Laboratory (Woods Hole, MA); and bullfrogs, Aquatic Facility Centre of Simon Fraser University (Burnaby, British Columbia, Canada). The animals were kept in aerated, flow-through water tanks under a 12-h light/dark cycle while experiments were being conducted. Fixed and fresh eyes from red-eared sliders were provided by C. Carr (University of Maryland, College Park, MD) and E. Enos (Marine Resources Centre), respectively. Fixed mouse eyes were obtained from staff at the Animal Care Facility of Simon Fraser University, and fixed eyes from Canada geese and green-winged teals (a species of northern duck) were provided by M. Juhas (Haida Gwaii Archipelago, British Columbia, Canada).

Laboratory animals were killed in a state of light or dark adaptation for histology or microspectrophotometry, respectively, and the retinas were processed as detailed in previous publications (Hárosi, 1987; Cheng et al., 2006; Novales Flamarique, 2011). All experimental procedures were approved by the Animal Care Committee of Simon Fraser University or the Marine Biological Laboratory, which are in compliance with the guidelines set by the Canadian Council for Animal Care and the National Institutes of Health.

Measurements

We obtained cell dimensions from live retinas (microspectrophotometry experiments) and from fixed, Epon-embedded retinas cut into thin (75 nm) sections and observed using a transmission electron microscope (model 7600; Hitachi; Fig. 1). These measurements were inner segment ellipsoid diameter (d_i), outer segment diameter at the base (d_o), outer segment diameter at a distance, z, from the base (d_z), and outer segment length and tip diameter when possible (Fig. 2). In addition, densities of rods and cones were obtained from thick (1 µm) histological sections.

Besides unpublished data, we obtained similar measurements from studies spanning the last 75 yr of anatomical literature. These included 116 species of fishes, covering the evolutionary spectrum from ancient groups like lampreys, elasmobranchs, and lungfishes to modern teleosts like killifishes, carps, and cichlids; 9 species of amphibians; 33 species of birds; 19 species of reptiles; 31 species of mammals; and 8 species of monotremes and marsupials. Table 1 details the species examined and the works consulted.

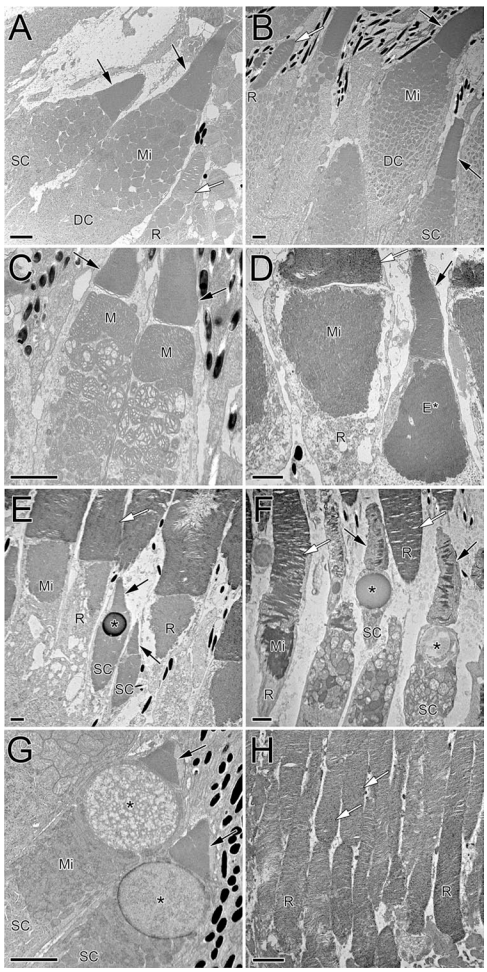

Figure 1. Electron micrographs of vertebrate photoreceptors illustrating diverse outer segment tapers and ellipsoid morphologies. (A) Goldfish single cone (SC) and rod (R) flanking one member of a double cone (DC). The cone ellipsoids are packed with mitochondria (Mi). Cone outer segments (black arrows) taper, whereas those of the rods do not (white arrow; only a portion of the rod outer segment is visible). (B) Single cone, double cone, and rod of coho salmon. In this species, there is a clear gradient in the size of cone mitochondria from smaller, at the level of the myoid, to larger, at the level of the ellipsoid. (C) Double cone from a mummichog killifish showing megamitochondria (M) associated with the ellipsoid of each double cone member. This species also has ellipsosomes, which arise from megamitochondria as the cristae disappear. (D) Rod and single cone from a bullfrog. The rod mitochondria are long and compacted; the single cone exhibits an ellipsosome-like structure (E*) in the ellipsoid. (E) Two single cones among rods in the bullfrog retina; one of the cones contains an oil droplet (*). Note the large difference in size between rods and cones. (F) Single cones and rods from a Canada goose. The single cones show different types of oil droplets. As in the frog, elongated mitochondria pack rod inner segments, and the mean diameter of cone ellipsoids (entrance aperture) is similar to that of rods. (G) Single cones of the red-eared slider turtle showing large oil droplets and pronounced cone taper. (H) Rods of the mouse retina. The cones in this and similar nocturnal species are hard to identify without molecular markers. Bars, 2 μm.

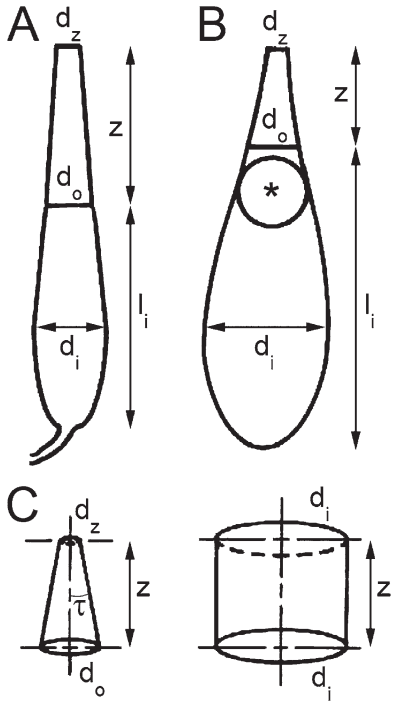

Figure 2. Drawings of single cones from fresh retinal preparations illustrating the morphological parameters measured as well as the taper angle, τ. The cellular dimensions were obtained from video images recorded via a microscope equipped with a calibrated infrared-sensitive video system. (A) Single cone from blue gill sunfish. (B) Single cone from leopard frog. (C) Cone outer segment (left) from B and an idealized representation of that of the optically equivalent rod (right). The equivalency is based on the assumption that both cells have equal entrance aperture with diameter d_i and that the cone ellipsoid funnels the incident flux to the outer segment without loss. The cellular dimensions (in μm) for these cones were as follows: (A) for the blue gill sunfish, $d_i = 8.3$, $d_o = 5.0$, $d_z = 2.9$, $z = 18$, and the inner segment length, $l_i = 25.2$; (B) for the leopard frog, $d_i = 7.2$, $d_o = 2.8$, $d_z = 1.3$, $z = 6.3$, and $l_i = 17.5$. The parameter z, in these two cases, equals the outer segment length, and d_z is the diameter at the tip of the outer segment. The asterisk in B depicts an oil droplet.

Each datum presented in the graphs of this study is the mean from a minimum of 15 cells for species used in live cell recordings (Table 2) and anywhere from three to thousands of cells for species data originating solely from the literature. Some publications failed to report cell numbers for the morphological data presented; in such cases, we took the numbers as averages for the entire retina. In our presentation of figures, we show parallel analyses for species for which measurements from live cells were obtained and those whose measurements originated from histological work, primarily from the published literature.

Methods to evaluate the first biophysical function

Evaluation of this function relied on a comparison of anatomically and physiologically derived measures of two parameters: characteristic length and taper, as described in Appendix 1. Two methods were used in the evaluation. The first involved the calculation of the required characteristic length, a_{h1}^{-1}, from Eq. 6 (Appendix 1) for each cell. The results were then compared with two separate estimates of characteristic length, $a_z'^{-1}$ and $a_z''^{-1}$, obtained with the aid of Eqs. 10 and 16 (Appendix 1). The necessary parameter values for the latter calculations were derived

TABLE 1

List of species for which literature data were obtained and sources

Common name	Scientific name	References
Fishes		
Narrow-mouthed lamprey	*Geotria australis*	Collin et al., 2003
South hemisphere lamprey	*Mordacia mordax*	Collin et al., 1999, 2004; Collin and Pottert, 2000
Sea lamprey	*Petromyzon marinus*	Dickson and Graves, 1979
River lamprey	*Lampetra japonica*	Ishikawa et al.,1987, 1989
Southern fiddler ray	*Trygonorhina fasciata*	Braekevelt, 1992a
Short tail stingray	*Dasyatis brevicaudata*	Braekevelt, 1994a
Blue spotted mask ray	*Dasyatis kuhlii*	Kohbara et al., 1987; Theiss et al., 2007
Giant shovelnose ray	*Rhinobatus typus*	Hart et al., 2004
Eastern shovelnose ray	*Aptychotrema rostrata*	Hart et al., 2004; Litherland and Collin, 2008
Sting ray	*Dasyatis sayi*	Hamasaki and Gruber, 1965
Electric ray	*Narcine brasilensis*	Ali and Anctil, 1974
Freshwater sting ray	*Paratrygon motoro*	Ali and Anctil, 1974
Red stingray	*Dasyatis akaiei*	Kohbara et al., 1987
Sepia stingray	*Urolophus aurantiacus*	Kohbara et al., 1987
Thornback ray	*Platyrhina sinensis*	Kohbara et al., 1987
Spiny dogfish	*Squalus acanthias*	Stell, 1972
Mediterranean dogfish	*Centroscysmus coelolepis*	Bozzano, 2004
Small spotted dogfish	*Scyliorhinus canicula*	Bozzanao et al., 2001
Black mouth dogfish	*Galeus mealstomus*	Bozzanao et al., 2001
Longsnout dogfish	*Deania eglantina*	Kohbara et al., 1987
Nurse shark	*Ginglymostoma cirratum*	Hamasaki and Gruber, 1965
Lemon shark	*Negaprion brevirostris*	Gruber et al., 1963
Great white shark	*Carcharodon carcharias*	Gruber et al., 1975; Gruber and Cohen, 1985
Mako shark	*Isurus oxyrinchus*	Gruber et al., 1975
Thresher shark	*Alopias vulpinus*	Gruber et al., 1975
Blue shark	*Prionace glauca*	Gruber et al., 1975; Kohbara et al., 1987
Banded houndshark	*Triakis scyllia*	Kohbara et al., 1987
Silky shark	*Carcharinus falciformis*	Gruber et al., 1975
White tip shark	*Carcharinus longimanus*	Gruber et al., 1975
Sandbar shark	*Carcharinus milberti*	Gruber et al., 1975
Brown bamboo shark	*Chiloscyllium punctatum*	Harahush et al., 2009
White tip reef shark	*Triaenodon obesus*	Litherland and Collin, 2008
Epaulette shark	*Hemiscyllium ocellatum*	Litherland and Collin, 2008
Ornate wobbegong	*Orectolobus ornatus*	Litherland and Collin, 2008
Australian lungfish	*Neoceratodus forsteri*	Bailes et al., 2006
South American lungfish	*Lepidosiren paradoxa*	Ali and Anctil, 1973
Coelacanth	*Latimeria chalumnae*	Locket, 1973
Green sturgeon	*Acipenser medirostru*	Sillman et al., 2005
Pallid sturgeon	*Scaphirhynchus albus*	Sillman et al., 2005
Siberian sturgeon	*Acipenser baeri*	Govardovskii et al., 1992
Amur sturgeon	*Acipenser shrenckii*	Fang et al., 2004
Shovelnose sturgeon	*Scaphirhynchus platorhynchus*	Sillman et al., 1999a
Paddlefish	*Polyodon spathula*	Sillman et al., 1999a; Sillman and Dahlin, 2004
Florida garfish	*Lepisosteus platyrhincus*	Collin and Collin, 1993
Bowfin	*Amia calva*	Ali and Anctil, 1976
Goldeye	*Hiodon alosoides*	Braekevelt, 1982
European eel	*Anguilla anguilla*	Braekevelt, 1984, 1985, 1988a,b
American eel	*Anguila rostrata*	Ali and Anctil, 1976
Northern anchovy	*Engraulis mordax*	Novales Flamarique, 2011
Goldfish	*Carassius auratus*	Stell and Hárosi, 1976
Carp	*Cyprinus carpio*	Bunt and Klock, 1980
Japanese dace	*Tribolodon hakonensis*	Hárosi and Hashimoto, 1983
Roach	*Leucisus rutilus*	Engström and Rosstorp, 1963; Zaunreiter et al., 1991

TABLE *(Continued)*

Common name	Scientific name	References
Tench	*Tinca tinca*	Douglas and Wagner, 1982
Zebrafish	*Danio rerio*	Nawrocki et al., 1985; Forsell et al., 2001; Kim et al.,2005
Cutlips minnow	*Exoglossum maxillingua*	Collin et al., 1996a
Silverjaw minnow	*Ericymba buccata*	Moore et al., 1950
Creek chub	*Semotilus atromaculatus*	Collin et al., 1996b
Gangfish	*Loregonus lavateus*	Reckel et al., 1999
Common white sucker	*Catostomus commersoni*	Novales Flamarique and Hárosi, 1997; Novales Flamarique and Hawryshyn, 1998
Razorback sucker	*Xyrauchen texanus*	Novales Flamarique et al., 2007
Channel catfish	*Ictalurus puntatus*	Sillman et al., 1993
White catfish	*Ictalurus catus*	Sillman et al., 1993
Brown bullhead	*Ictalurus nebulosus*	Welsh and Osborn, 1937; Ali and Anctil, 1976
Coho salmon	*Oncorhynchus kisutch*	Cheng et al., 2006, 2007
Chum salmon	*Oncorhynchus keta*	Cheng et al., 2006
Pink salmon	*Oncorhynchus gorbuscha*	Cheng et al., 2006
Chinook salmon	*Oncorhynchus tschawytscha*	Cheng et al., 2006
Atlantic salmon	*Salmo salar*	Novales Flamarique, 2002, 2011; Cheng et al., 2006
Rainbow trout	*Oncorhynchus mykiss*	Kusmic and Gualtieri, 2000; Cheng and Novales Flamarique, 2007; Cheng et al., 2007, 2009
Smelt	*Osmerus eperlanus*	Reckel et al., 2003
Salamander fish	*Lepidogalaxias salamandroides*	Collin and Collin, 1998
Waryfish	*Scopelosaurus lepidus*	Munk, 1977
Greenland cod	*Gadus ogac*	Ali and Anctil, 1976
Antarctic cod	*Dissostichus mawsoni*	Meyer-Rochow and Klyne, 1982
Bald rock cod	*Trematomus borchgrevinki*	Meyer-Rochow and Klyne, 1982
Emerald rock cod	*Trematomus bernacchii*	Meyer-Rochow and Klyne, 1982
Common cod	*Gadus callarias*	Engström, 1961
Burbot	*Lota lota*	Engström, 1961
Tadpole fish	*Raniceps raninus*	Engström, 1961
Silver hake	*Merluccius bilinearis*	Ali and Anctil, 1976
Capelin	*Mallotus villosus*	Ali and Anctil, 1976
Mummichog killifish	*Fundulus heteroclitus*	Anctil and Ali, 1976; Novales Flamarique and Hárosi, 2000
Mangrove killifish	*Rivulus marmoratus*	Ali et al., 1989
Four-eyed fish	*Anableps anableps*	Borwein and Hollenberg, 1973
Guppy	*Lebistes reticulatus*	Müller, 1952; Yacob et al., 1977; MacNichol et al., 1978; Kunz et al., 1983
Pipefish	*Corythoichthyes paxtoni*	Collin and Collin, 1999
Halfbeak	*Dermogenys pusillus*	Reckel et al., 2002; Reckel and Melzer, 2003
Australian rainbowfish	*Melanotaenia maccullochi*	Reckel et al., 2002; Reckel and Melzer, 2003
Celebes rainbowfish	*Marosatherina ladigesi*	Reckel et al., 2002; Reckel and Melzer, 2003
Sea needle	*Belone belone*	Reckel et al., 2001, 2002; Reckel and Melzer, 2003
Lesser weever	*Trachinus vipera*	Kunz et al., 1985
European perch	*Perca fluviatilis*	Ahlbert, 1973; Guma'a, 1982
Yellow perch	*Perca flavescens*	Ali and Anctil, 1976
Green sunfish	*Lepomis cyanellus*	Burnside and Ackland, 1984; Dearry and Barlow, 1987
Butterfly fish	*Pantodon buchholzi*	Braekevelt, 1990a
Black bream	*Acanthopagrus butcheri*	Shand et al., 1999
Blackstriped cardinalfish	*Apogon angustatus*	Fishelson et al., 2004
Iridescent cadinalfish	*Apogon kallopterus*	Fishelson et al., 2004
Yellowstriped cardinalfish	*Apogon cyanosoma*	Fishelson et al., 2004
Cook's cardinalfish	*Apogon cookie*	Fishelson et al., 2004
Rock bass	*Ambloplites rupestris*	Munz and McFarland, 1977
Large-mouth bass	*Micropterus salmoides*	García and de Juan, 1999
Striped bass	*Morone saxatilis*	Paillart et al., 2006
West Australian dhufish	*Glaucosoma hebraicum*	Shand et al., 2001
Black sea bass	*Centropristis striata*	Singarajah and Hárosi, 1992

TABLE *(Continued)*

Common name	Scientific name	References
Snake mackerel	*Gempylus serpens*	Munk, 1985
Walleye	*Stizosteidon vitreum vitreum*	Zyznar and Ali, 1975; Januschka et al., 1987
Sauger	*Stizosteidon canadense*	Ali and Anctil, 1977
Nile tilapia	*Oreochromis niloticus*	Braekevelt et al., 1998
Golden dwarf cichlid	*Nannacara anomala*	Wagner, 1978; Douglas and Wagner, 1982
Velvet cichlid	*Astronotus ocellatus*	Braekevelt, 1992b
Burton's haplochromis	*Haplochromis burtoni*	Pietzsch-Rohrschneider, 1976
Goldsinny wrasse	*Ctenolabrus suillus*	Engström, 1963
Corkwing wrasse	*Crenilabrus melops*	Engström, 1963
Winter flounder	*Pseudopleuronectes americanus*	Evans and Fernald, 1993
Amphibians		
African clawed frog	*Xenopus laevis*	Kinney and Fisher, 1978a,b; Hollyfield et al., 1984; Röhlich et al., 1989; Röhlich and Szél, 2000
Leopard frog	*Rana pipiens*	Nilsson, 1965
Bullfrog	*Rana catesbeiana*	Hisatomi et al., 1998
Edible frog	*Rana esculenta*	Reichenbach and Fuchs, 1983
Tropical toad	*Bufo marinus*	Moody and Robertson, 1960; Hárosi, 1975
Tiger salamander	*Ambystoma tigrinum*	Hárosi, 1975; Mariani, 1986; Braekevelt, 1993a; Sherry et al., 1998; Ma et al., 2001
Axotol	*Ambystoma mexicanum*	Custer, 1973
Red-back salamander	*Plethodon cinereus*	Braekevelt, 1992c
Newt	*Triturus viridescens*	Keefe, 1971
Birds		
Chicken	*Gallus domesticus*	Meyer and May, 1973; Araki et al., 1984; Szél et al., 1986; Oishi et al., 1990
Pigeon	*Columba livia*	Cohen, 1963; Mariani and Leure-duPree, 1978; Cserháti et al., 1989
Crow	*Corvus brachyrhynchos*	Braekevelt, 1994b
Great blue heron	*Ardea Herodias*	Rojas et al., 1999a
Yellow-crowned heron	*Nycticorax violaceus*	Rojas et al., 1999a
Black-crowned heron	*Nycticorax nycticorax*	Gondo and Ando, 1995
Cattle egret	*Bubulcus ibis*	Rojas et al., 1999a
Tricolored egret	*Egretta tricolor*	Rojas et al., 1999a
American white ibis	*Eudocimus ruber*	Rojas et al., 1999a
Roseate spoonbill	*Ajaia ajaja*	Rojas et al., 1999a
Wilson's plover	*Charadrius wilsonia*	Rojas et al., 1999b
Short-billed dowitcher	*Limnodromus griseus*	Rojas et al., 1999b
American woodcock	*Scolopax minor*	Rojas et al., 1999b
Black-winged stilt	*Himantopus himantopus*	Rojas et al., 1999b
Willet	*Catoptrophorus semipalmatus*	Rojas et al., 1999b
Red-tailed hawk	*Buteo jamaicensis*	Braekevelt, 1993b
Great horned owl	*Bubo virginianus*	Braekevelt, 1993c
Barred owl	*Strix varia*	Braekevelt et al., 1996
Mallard duck	*Anas platyrhynchos*	Braekevelt, 1990b
Australian galah	*Eolophus roseicapillus*	Braekevelt and Richardson, 1996
Emu	*Dromaius novaehollandiae*	Braekevelt, 1998
Japanese quail	*Coturnix coturnix japonica*	Konishi, 1965; Oishi et al., 1990; Rojas et al., 2007
Eastern tree sparrow	*Passer montanus*	Gondo and Ando, 1995
House swallow	*Hirundo rustica*	Gondo and Ando, 1995
Great tit	*Parus major*	Engström, 1958
American robin	*Turdus migratorius*	McNeil et al., 2005
Hermit thrush	*Catharus guttatus*	McNeil et al., 2005
Mourning dove	*Zenaida macroura*	McNeil et al., 2005
Common grackle	*Quiscalus quiscula*	McNeil et al., 2005
Oil bird	*Steatoinis caripensis*	Martin et al., 2004; Rojas et al., 2004
Common pauraque	*Nyctidromus albicellis*	Rojas et al., 2004

TABLE *(Continued)*

Common name	Scientific name	References
Ring billed gull	*Larus delawarensis*	Emond et al., 2006
Gray gull	*Larus modestus*	Emond et al., 2006
Reptiles		
Red-eared slider	*Pseudemys scripta elegans*	Baylor and Fettiplace, 1975; Leeper, 1978; Kolb and Jones, 1982, 1987; Ohtsuka and Kawamata, 1990
Snapping turtle	*Chelydra serpentina*	Baylor and Fettiplace; 1975; Leeper; 1978
Reeve's turtle	*Geoclemys reevesii*	Ohtsuka, 1985; Ohtsuka and Kawamata; 1990
Garter snake	*Thamnophis sirtalis*	Wong; 1989; Sillman et al., 1997
Ball python	*Python regius*	Sillman et al., 1999b
Common boa	*Boa constrictor imperator*	Sillman et al., 2001
Mississippi alligator	*Alligator mississippiensis*	Kalberer and Pedler, 1963; Sillman et al., 1991
Caiman	*Caiman crocodilus*	Govardovskii et al., 1988
Tokay gecko	*Gekko gecko*	Pedler and Tilly, 1964; Crescitelli, 1972
Blue-tailed day gecko	*Phesulma inunguis*	Pedler and Tansley, 1963; Pedler and Tilly, 1964
Coastal banded gecko	*Coleonyx variegates*	Dunn, 1966
Mediterranean gecko	*Hemydactilus turcicus*	Pedler and Tilly, 1964; Loew et al., 1996
House gecko	*Hemydactilus garnotii*	Loew et al., 1996
Scinc gecko	*Teratoscincus scincus*	Govardovskii et al., 1984; Loew et al., 1996
Chameleon	*Chamaleo chamaleo*	Armengol et al., 1981
Western fence lizard	*Sceloporpus occidentalis*	Young, 1977; Bernstein et al., 1984
Ornate dragon lizard	*Ctenophorus ornatus*	Barbour et al., 2002
Tuatara	*Sphenodon punctatu*	Meyer-Rochow et al., 2005
Bouton's skink	*Cryptoblepharus boutonii*	Röll, 2001
Mammals		
Stumptail macaque	*Macaca arctoides*	Hoang et al., 2002
Rhesus monkey	*Macaca mulatta*	Cohen, 1961; Leach, 1963; Dowling, 1965; Young, 1971; Borwein et al., 1980
Crab-eating macaque	*Macaca fascicularis*	Borwein et al., 1980
Pigtail macaque	*Macaca nemestrina*	Packer et al., 1989
Owl monkey	*Aotes trivirgatus*	Jones, 1965; Murray et al., 1973; Ogden, 1975
Vervet monkey	*Cercopithecus aethiops*	Braekevelt, 1987
Human	*Homo sapiens*	Missotten, 1966; Dieterich and Rohen, 1970; Steinberg et al., 1977; Curcio et al., 1990; Hoang et al., 2002
Dog	*Canis domesticus*	Shively et al., 1970; Hebel, 1971
Wolf	*Canis lupus*	Peichl et al., 2001
Cat	*Felis domesticus*	Steinberg et al., 1973; Braekevelt, 1990c
Ferret	*Mustela putorius furo*	Braekevelt, 1983a
Mink	*Mustela vison*	Dubin and Turner, 1977; Braekevelt, 1990d
Spotted hyena	*Crocuta crocuta*	Calderone et al., 2003
Rabbit	*Oryctologus cuniculus*	Szél et al., 1988
Cow	*Bos taurus*	Szél et al., 1988
Pig	*Sus scrofa domesticus*	Szél et al., 1988; Hendrickson and Hicks, 2002
Domestic sheep	*Ovis aries*	Braekevelt, 1983b
Mouflon	*Ovis musimon*	Peichl, 2005
Long-finned pilot whale	*Globicephala melaena*	Peichl et al., 2001
13-lined squirrel	*Spermophilus tridecemlineatus*	West and Dowling, 1975; Anderson and Fisher, 1976
Mexican ground squirrel	*Spermophilus mexicanus*	West and Dowling, 1975; Anderson and Fisher, 1976
California ground squirrel	*Spermophilus beecheyi*	Anderson and Fisher, 1976
Eastern gray squirrel	*Sciurus carolinensis*	Cohen, 1964; West and Dowling, 1975; Anderson and Fisher, 1976
Western gray squirrel	*Sciurus griseus*	Anderson and Fisher, 1976
Prairie dog	*Cynomys ludovicianus*	West and Dowling, 1975
Mouse	*Mus musculus*	Carter-Dawson and LaVail, 1979
Tree shrew	*Tupaia belangeri*	Kühne, 1983; Foelix et al.,1987; Müller and Peichl, 1989; Petry and Hárosi, 1990; Petry et al., 1993; Knabe et al., 1997
African giant rat	*Cricetomys gambianus*	Peichl, 2005

TABLE *(Continued)*

Common name	Scientific name	References
Madagascar rousette	*Rousettus madagascariensis*	Müller et al., 2007
Seba's short-tailed bat	*Carollia perspicillata*	Müller et al., 2009
Greater horseshoe bat	*Rhinolophus ferrumequinum*	Kim et al., 2008
Monotremes and marsupials		
Echidna	*Tachyglossus aculeatus*	Young and Pettigrew, 1991
Fat-tailed dunnart	*Sminthopsis crassicaudata*	Arrese et al., 2002, 2003
Honey possum	*Tarsipes rostratus*	Arrese et al., 2002, 2003
Mouse opossum	*Thylamis elegans*	Palacios et al., 2010
Tammar wallaby	*Macropus eugenii*	Hemmi and Grünert, 1999
Quokka	*Setonix brachyurus*	Arrese et al., 2005
Quenda	*Isoodon obesulus*	Arrese et al., 2005
Agouti	*Dasyprocta aguti*	Rocha et al., 2009

In the case of the northern anchovy, only retinal areas with regular cones were evaluated (Novales Flamarique, 2011).

from previous determinations performed on equivalent cells. For example, it was assumed that cones with vitamin A_2–type pigments share the properties with those of the yellow perch, goldfish, or Japanese dace and have the following parameter values: ε = 30,000 liter mol^{-1} cm^{-1}, c = 3.5 mM, R = 2.2, and $S_\perp$ = 0.0125 μm^{-1}. For cones using vitamin A_1–type pigments, ε = 42,000 liter mol^{-1} cm^{-1}, c = 3.5 mM, R = 2.5, and $S_\perp$= 0.0175 μm^{-1} (Hárosi and MacNichol, 1974; Hárosi, 1975, 1976, 1984, 1985; Hárosi and Hashimoto, 1983). The estimated characteristic lengths were not significantly affected by the particular values assumed for individual parameters. For instance, we could have used Liebman and Granda's (1971) specific absorbance of 0.0130 μm^{-1} to obtain $a_z''^{-1}$ = 33.4 μm or assumed 3-mM pigment concentration and an infinite dichroic ratio (k = 1.5), as did Hodgkin and O'Bryan (1977), and arrived at $a_z'^{-1}$ = 32.2 μm. These values are similar to those reported in Table 2.

As a second method for testing the validity of the first function, we calculated a new diameter (d_z') for each cell that would occur at critical taper by using a_z' and the rest of the geometrical data in Eq. 5 (Appendix 1). The actual taper, τ, obtained with d_z, was then recalculated using d_z' in Eq. 17. The resulting τ' represents taper for each cell that would satisfy invariance of flux density along the outer segment.

Evaluation of the second biophysical function

Eq. 30 of Appendix 2 is an expression for the signal-to-noise ratio along an outer segment. This equation was scrutinized to assess the validity of the second proposed function.

Evaluation of the third biophysical function

For the lack of a compact theoretical expression (Appendix 3), this function could not be verified experimentally. Our approach here was to test whether several morphological observations across phyla were consistent with it. For instance, the difference in light-gathering efficiency by tapered versus nontapered photoreceptors (Appendix 3) led us to predictions about the rod/cone ratios of primarily diurnal animals; i.e., animals with both diurnal and crepuscular/nocturnal rhythms, but in which the primary rhythm is diurnal, and in which utilization of both cone and rod pathways occurs during the day (these species are to be contrasted with those that are fully diurnal, e.g., some ground squirrels [West and Dowling, 1975; Anderson and Fisher, 1976], or primarily nocturnal, e.g., the giant African rat; Peichl, 2005). In addition, we postulated that there should be a correlation between outer segment taper and ellipsoid concentration factor (Eq. 33, Appendix 3), the latter being a measure of the ability to concentrate light from inner to outer segment. To test this, we used critical taper (Appendix 1) as a benchmark and expressed actual taper as the ratio $a_z'^{-1}/a_{h1}^{-1}$, indicating how many critical characteristic lengths would equal the characteristic length considered realistic.

RESULTS

Cone taper exceeds critical taper

Table 2 presents typical morphometric data obtained from live photoreceptors during microspectrophotometric experiments, in this case from individual photoreceptors of goldfish. Values of derived variables (e.g., taper, characteristic length, and concentration factor) are also presented. Figs. 3–6 show means from analogous datasets for the various species examined.

Comparison of data in columns 8–10 of Table 2 reveals that the characteristic length corresponding to critical taper differs from the characteristic length calculated from known data. Moreover, the difference in most cases goes far beyond the margin of error (~0.1 μm, from repeated measures). Except for one cone (Table 2, row 1) that came close to having critical taper, the a_{h1}^{-1} values for the rest of the cones are much smaller than expected. A smaller characteristic length, however, means a larger absorption coefficient. We can consider, for instance, the blue-absorbing single cone on line 25 of Table 2. For it to have critical taper, the axial extinction would have to be ~3.8-fold higher than a realistic value.

As is apparent from columns 6 and 7 of Table 2, the taper of real cones is excessive. For the vast majority of species studied, whether the data originated from live cell measurements (Fig. 3 A) or from fixed, histological material (Fig. 3 B), the mean cone taper (τ) was at least 1.5 times the critical taper (τ'). Only in the case of bats, the giant African rat, and foveal-perifoveal cones of primate retinas was cone taper statistically the same as critical taper ($P > 0.05$, paired *t* tests). On average, the ratio τ/τ' ± SD was 4.8 ± 2.4 for fishes, 5.1 ± 1.7 for amphibians,

TABLE 2

Measured parameters and computed variables from fresh preparations of goldfish retina used in microspectrophotometry experiments

Cell type	d_i	d_o	d_z	z	τ	τ'	a_{h1}^{-1}	$a_z'^{-1}$	$a_z''^{-1}$	$a_z'^{-1}/a_{h1}^{-1}$	F_c
	μm	μm	μm	μm	^{o}	^{o}	μm	μm	μm		
DC_1-R	8.9	6.1	4.6	18.3	2.3	2.26	32.4	33.8	34.7	1.04	2.12
DC_1-G	8.4	5.3	3.0	18.3	3.6	1.97	16.1	33.8	34.7	2.10	2.51
DC_2-R	9.6	6.9	4.6	19.8	3.3	2.53	24.4	33.8	34.7	1.38	1.93
DC_2-G	9.1	6.1	3.8	12.2	5.4	2.36	12.9	33.8	34.7	2.62	2.22
DC_3-R	9.4	6.9	4.6	13.7	4.8	2.64	16.9	33.8	34.7	2.00	1.85
DC_3-G	8.8	6.1	4.6	10.7	4.0	2.39	19.0	33.8	34.7	1.78	2.08
DC_4-R	9.2	4.6	3.0	10.7	4.3	1.80	12.5	33.8	34.7	2.70	4.00
DC_4-G	9.8	6.1	4.6	7.6	5.6	2.44	13.5	33.8	34.7	2.51	2.58
DC_5-R	9.1	5.4	2.9	19.6	3.6	2.00	15.8	33.8	34.7	2.14	2.84
DC_5-G	8.4	6.9	4.1	21.4	3.7	2.50	20.5	33.8	34.7	1.64	1.48
DC_6-R	9.2	7.6	4.7	19.4	4.3	2.79	20.2	33.8	34.7	1.67	1.46
DC_6-G	8.1	6.8	4.5	18.3	3.6	2.52	22.1	33.8	34.7	1.52	1.41
DC_7-R	6.5	3.8	2.4	12.9	3.1	1.46	14.0	33.8	34.7	2.41	2.92
DC_7-G	6.4	3.3	2.1	12.3	2.8	1.28	13.6	33.8	34.7	2.48	3.76
DC_8-R	8.3	5.5	3.7	13.3	3.9	2.11	16.8	33.8	34.7	2.01	2.28
DC_8-G	7.8	5.2	3.6	12.8	3.6	2.01	17.4	33.8	34.7	1.94	2.25
DC_9-R	8.7	5.8	3.5	18.2	3.6	2.15	18.0	33.8	34.7	1.88	2.25
DC_9-G	8.4	6.1	4.2	19.4	2.8	2.24	26.0	33.8	34.7	1.30	1.89
DC_{10}-R	10.2	7.6	4.5	18.4	4.8	2.82	17.6	33.8	34.7	1.93	1.80
DC_{10}-G	9.6	7.2	4.6	17.4	4.3	2.69	19.4	33.8	34.7	1.74	1.77
SC_1-R	9.1	6.1	3.8	15.2	4.3	2.31	16.1	33.8	34.7	2.10	2.22
SC_2-R	8.8	6.1	3.8	16.7	3.9	2.29	17.6	33.8	34.7	1.92	2.08
SC_3-R	6.2	4.5	3.0	12.6	3.4	1.74	15.5	33.8	34.7	2.17	1.89
SC_4-R	8.2	4.1	2.8	12.8	2.9	1.58	16.8	33.8	34.7	2.01	4.00
SC_5-B	9.3	6.1	3.8	8.4	7.8	2.43	8.87	33.8	34.7	3.81	2.32
SC_6-B	9.4	6.1	4.6	7.6	5.6	2.44	13.5	33.8	34.7	2.51	2.37
SC_7-B	9.2	6.5	4.8	12.2	4.0	2.52	20.1	33.8	34.7	1.68	2.00
SC_8-B	9.3	6.2	4.1	14.8	4.1	2.36	17.9	33.8	34.7	1.89	2.25
SC_9-B	8.8	5.8	3.9	13.6	4.0	2.22	17.1	33.8	34.7	1.97	2.30
SC_{10}-B	8.7	6.1	3.6	10.1	7.1	2.40	9.58	33.8	34.7	3.53	2.03
Rod_1	2.2	2.2	2.1	42.0	0.1	0.69	451	33.8	34.7	0.07	1.00
Rod_2	2.0	2.0	2.0	39.1	0.0	0.64	∞	33.8	34.7	0.00	1.00
Rod_3	2.1	2.1	2.0	38.4	0.1	0.67	389	33.8	34.7	0.09	1.00
Rod_4	2.3	2.3	2.3	44.0	0.0	0.71	∞	33.8	34.7	0.00	1.00
Rod_5	1.9	1.8	1.8	36.6	0.0	0.59	∞	33.8	34.7	0.00	1.11
Rod_6	1.9	1.9	1.9	39.7	0.0	0.60	∞	33.8	34.7	0.00	1.00
Rod_7	2.1	2.0	2.0	40.3	0.0	0.63	∞	33.8	34.7	0.00	1.10
Rod_8	2.2	2.1	2.1	41.3	0.0	0.67	∞	33.8	34.7	0.00	1.10
Rod_9	2.0	2.0	2.0	43.5	0.0	0.62	∞	33.8	34.7	0.00	1.00
Rod_{10}	1.9	1.7	1.7	35.5	0.0	0.57	∞	33.8	34.7	0.00	1.25
Rod_{11}	2.2	2.2	2.2	38.0	0.0	0.71	∞	33.8	34.7	0.00	1.00
Rod_{12}	2.1	2.0	2.0	37.7	0.0	0.65	∞	33.8	34.7	0.00	1.10
Rod_{13}	2.2	2.2	2.2	41.8	0.0	0.70	∞	33.8	34.7	0.00	1.00

DC, double cone; SC, single cone. R, G, and B indicate the presence of visual pigments with maximum wavelength of absorption in the red (LWS opsin), green (RH2 opsin), or blue (SWS2 opsin) regions of the spectrum.

5.5 ± 2.1 for birds, 5.7 ± 3.8 for reptiles, 4.6 ± 3.2 for mammals, and 4.3 for marsupials (two species). Among the fishes, the mean elasmobranch ratio (7.2 ± 2.7) was about twice that of teleosts (3.8 ± 1.4), and the highest ratios among the teleosts were for lungfishes (5.2) and killifishes (4.8), which, like most amphibians, reptiles, and birds and some fishes and monotremes, have oil droplets (lungfishes) or have ellipsosomes (killifishes) in the ellipsoid region (Fig. 1). Among the reptiles, the ratio for the strictly diurnal garter snake (5.3) was about half that of primarily nocturnal snakes like the boa and ball python (mean of ~11). Overall, phylogenetic

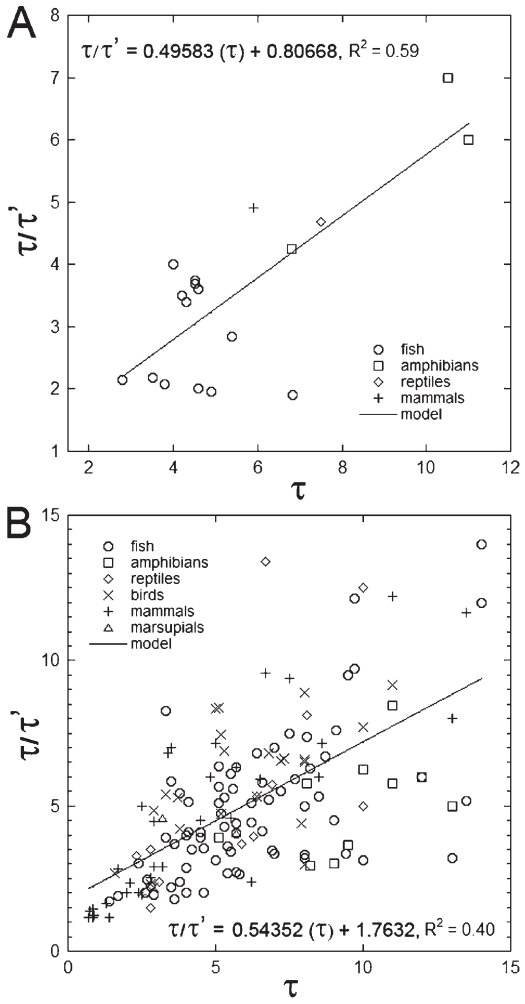

Figure 3. Ratio of observed taper to critical taper (τ/τ') in relation to observed taper (τ). (A) Species from which live cell measurements were obtained. (B) Species for which measurements originated from the literature. Recall that taper is defined as the angle between the axis of the cone and the inclination of the contour line, which, upon precession, describes the conical surface. Critical taper is the taper required to exactly compensate for light flux diminution by absorption (self-screening) so that flux density remains invariant throughout the outer segment. In general, taper was highest for species with focusing organelles in the ellipsoids.

groups with focusing structures in the ellipsoids (e.g., oil droplets, microdroplets, and megamitochondria) had larger τ/τ' ratios than those lacking them.

Both methods of assessment led to the same general observation: overall, cones are more tapered than they ought to be for critical taper. Therefore, cone outer segment taper overcompensates for the loss of signal caused by self-screening. In contrast, rod outer segments, if tapered at all, have less than critical taper (Table 2), with the potential exception of rods in lampreys and geckos, species in which the two photoreceptor types are hard to classify because they exhibit intermediate morphological and molecular attributes (Collin et al., 2004; Muradov et al., 2008; Zhang et al., 2006).

Signal-to-noise ratio increases beyond that predicted by critical taper

Examination of Eq. 30 (Appendix 2) reveals the following: (a) when A_z is invariant in z (cylindrical outer segment), the signal-to-noise ratio, S/N, diminishes exponentially along z as a result of self-screening; (b) if A_z versus z diminishes by tapering, the S/N will undergo proportionate increases; (c) for critical taper, when A_z varies in accordance with Eq. 4 (Appendix 1), the exponential terms cancel, and the S/N becomes independent of z. From Eq. 30 we can also deduce that, for excessive taper, i.e., when a cone cross section (A_z) diminishes faster than the exponential fall-off of signal, the signal-to-noise ratio may actually increase toward the apex of a cone outer segment. Eq. 30 thus reveals an important tendency: more taper means greater improvement in the signal-to-noise ratio along an outer segment. For this reason, in the absence of other requirements, cones should taper as much as possible.

Inner segment morphology as a major determinant of outer segment taper

For the lack of a compact theoretical expression (see Appendix 3), the third function linking inner segment morphology to outer segment taper could not be verified experimentally. Nevertheless, several observations were consistent with it, as demonstrated by the following analyses using examples from diverse phylogenetic groups.

Teleosts, like the goldfish, have typically large, plump inner segments and shorter outer segments compared with the rods (Fig. 1). The average goldfish cone in this study had an entrance aperture (assumed to be equal to the broadest region of the ellipsoid) of 8.7-µm diameter, wherefrom light would be funneled to the base of the outer segment with a mean diameter of 5.9 µm (Table 2). The concentration factor, F_C, by Eq. 33 (Appendix 3) is 2.2. The outer segment volume calculated by Eq. 34 yields 277 μm^3. The volume of a cylinder with equal base diameter is 399 μm^3. Their ratio gives 1.4 for the geometry factor, F_G, by Eq. 35. Additionally, the volume reduction ratio, V_R, is obtained at 3.1 by Eq. 36. Thus, the cone outer segment uses ~32% of the volume of that of the hypothetical optically equivalent rod. The rod cells measured in these goldfish preparations were quite uniform, with an average outer segment diameter of 2.1 µm and lengths in the range of 36–44 µm. For a 40-µm-long rod outer segment, we can calculate the axial absorptance by Eqs. 3 and 22 using a_z' (Appendix 1). Accordingly, such a rod would absorb ~69% of the light incident at its base. By a similar calculation, the 15-µm-long cone outer segment would absorb only 35% of the flux it receives. Therefore, the rod is the better light detector of the two. However, this rod collects a mere fraction of what a single cone can gather from the retinal illumination. In fact, it would take $(8.7/2.1)^2 = 17.2$ rods

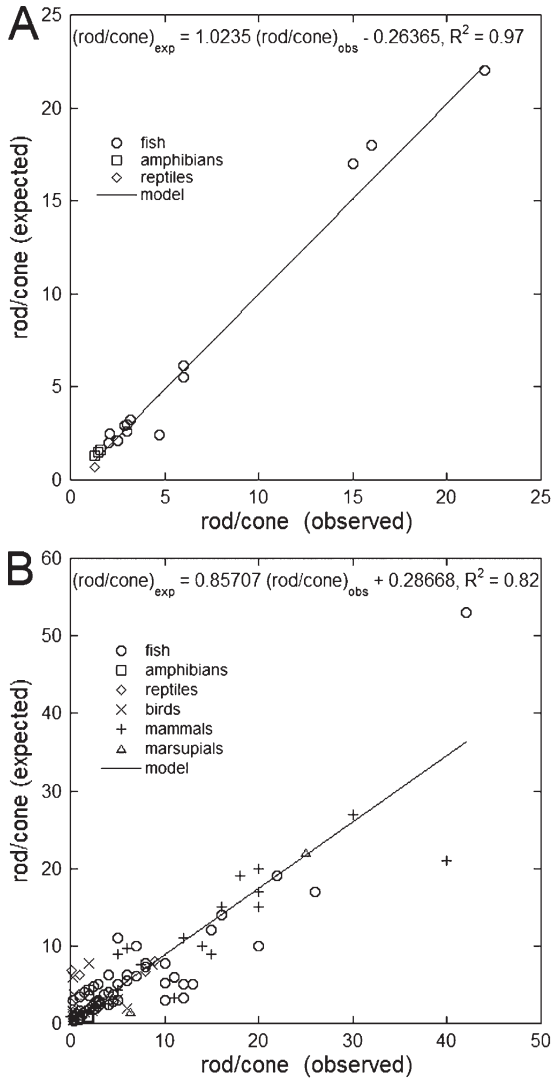

Figure 4. Regressions of expected rod/cone ratios as a function of those observed for primarily diurnal (though birythmic) species. (A) Data for species from which live cell measurements were obtained. (B) Data for species for which measurements originated from the literature.

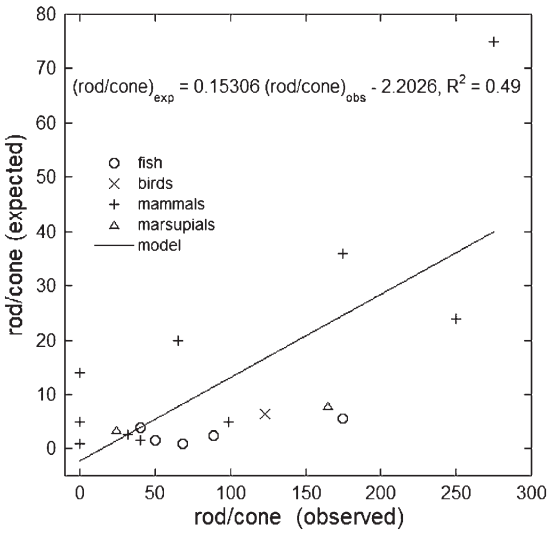

Figure 5. Regression of expected rod/cone ratios as a function of those observed for fully diurnal and primarily nocturnal species. Data originated from the literature.

to intercept as much incident flux as the average cone considered here. The rod/cone ratio in goldfish was reported to be 15:1 (Stell and Hárosi, 1976). The reasonably satisfactory agreement between predicted and observed ratios suggests that, in this animal, interception of equal light flux, a property linked to inner segment aperture, appears to be the criterion driving rod and cone densities.

When this analysis was applied to the other, predominantly diurnal, species studied, the correlations between observed and expected rod/cone ratios were surprisingly good (Fig. 4, A and B). On average, the rod/cone ratio expected and observed ± SD for the various phylogenetic groups were as follows: 6.9 ± 10 and 7.6 ± 9.2 (fishes), 1.4 ± 1.6 and 1.5 ± 0.58 (amphibians), 2.0 ± 2.1 and 1.4 ± 2.0 (birds), 5.0 ± 3.4 and 6.8 ± 7.4 (reptiles), 12 ± 7.4 and 13 ± 10 (mammals), and 12 and 16 (marsupials, two species). Among the fishes, the rod/cone ratios of teleosts were better predicted than those of elasmobranchs; the mean predicted and observed ratios for these two groups were 6.2 ± 9.0 and 6.4 ± 9.1 (teleosts) and 8.5 ± 12 and 10 ± 9.1 (elasmobranchs). Overall, the highest rod/cone ratios occurred for the walleye (a teleost with "remarkably large cones"; Januschka et al., 1987) and the mink. The best predictions occurred within the teleosts and mammals, especially for primates (predicted and expected mean rod/cone ratios were 16 ± 7.3 and 17 ± 8.8). The worst predictions (i.e., ratio of expected to predicted, or vice versa, >2) occurred within the birds (owls) and reptiles (snakes) as well as for elasmobranchs and one teleost, the snake mackerel. Some of these animals (e.g., owls, several species of elasmobranchs, and large snakes) were included in the analysis because of reported crepuscular (cone driven) activity, although they may be primarily nocturnal and perhaps not very appropriate for inclusion in these regressions. Indeed, the rod/cone ratios of primarily nocturnal or fully diurnal animals are not very well predicted based on our principle of equal flux sharing between photoreceptor types (Fig. 5). Primarily nocturnal or dark habitat–dwelling species, which include deep ocean sharks and eels, several mammals (e.g., the mouse, African giant rat, bats, and the spotted hyena), the oil bird, and marsupials (opossums and the tammar wallaby), have large to very large rod/cone ratios (some exceeding 100:1). At the other end of the spectrum, strictly diurnal species like some ground squirrels, the prairie dog, and the tree shrew have very small rod/cone rations (≤0.1). None of these species, located at either extreme of the rod/cone ratio range, were included in the analysis leading to Fig. 4 B.

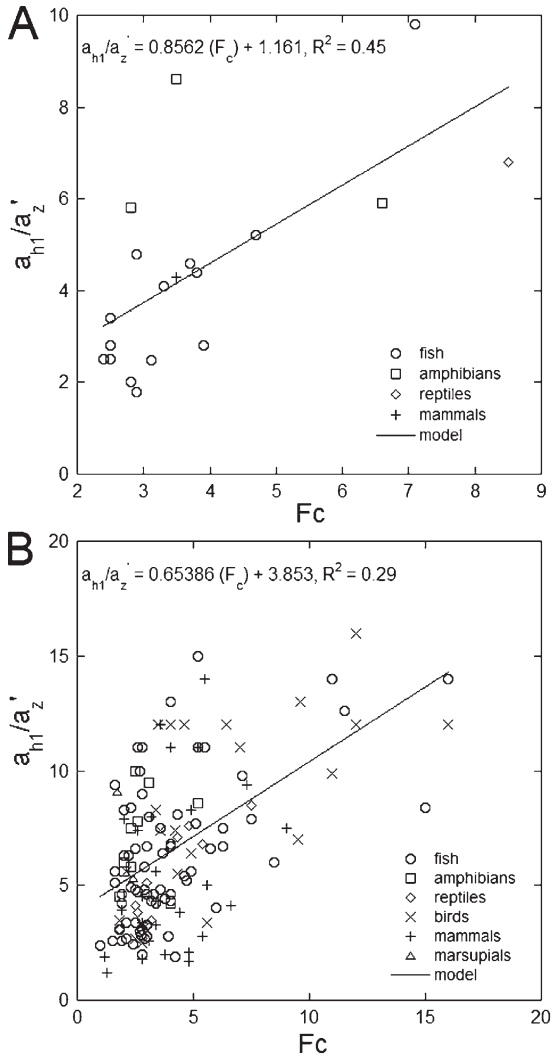

Figure 6. Regressions of the ratio of realistic to critical characteristic length ($a_z'^{-1}/a_{h1}^{-1}$) as a function of concentration factor (F_C). Recall that the characteristic length is the distance along the outer segment at which the light flux, Φ, falls to 0.368 of the incident light flux at the base, Φ_o. The concentration factor is the square of the ratio between ellipsoid diameter at its largest cross section and outer segment base diameter, i.e., $F_C = (d_i/d_o)^2$, and represents coupling of light flux without loss from ellipsoid to outer segment. (A) Data for species from which live cell measurements were obtained. (B) Data for species for which measurements originated from the literature.

In contrast to the comparable size of photoreceptors in teleosts and mammals, the retinas of amphibians have colossal rods and minute cones (Fig. 1). The dichotomy in outer segment size is seldom as pronounced as in frog species, with the possible exception of the salamanders (Crescitelli, 1972). However, even in these animals, the important feature determining rod and cone densities appears to be the equal sampling of the plane, where, presumably, the image of the outside world is formed within the eye.

As an example, the mean cone ellipsoid diameter (entrance aperture) of the African clawed frog was found to be 7 μm, whereas the mean diameter of the outer segment base was 2.9 μm. Repeating the procedure used previously, we can calculate, by using Eqs. 33–36 (Appendix 3), the following: $F_C = 5.8$, $V_c = 20.1\ \mu m^3$, $V_r = 39.6\ \mu m^3$, $F_G = 1.97$, and $V_R = 11.4$. The optically equivalent cylinder, as indicated in Fig. 2 C, has a volume of $\sim$231 μm^3. Thus, the cone outer segment volume is only $\sim$9% of that of the cylinder.

The preparations where frog single cones were located also had rhodopsin-containing red rods with an outer segment diameter equal to the widest region of the ellipsoid, with a mean diameter of 7 μm. This finding may be interpreted in terms of the cone ellipsoid's light-gathering property and suggests that the entrance aperture of single cones and red rods are equal in frogs. Further support for the idea of equal flux collection by these cells in the frog retina can be found in the electron microscopic studies of Nilsson (1964, 1965). He showed, among other things, that red rods and single cones have about equal areas in cross section at the inner segment level (Nilsson, 1964). These photoreceptors, therefore, may indeed gather nearly equal fluxes from a uniform retinal illumination.

The actual volume of a red rod outer segment (at a length of 66 μm) is $\sim$2,500 μm^3. Using known parameters and Eqs. 3 and 22 (Appendix 1), we can calculate that these rods may catch 94% of axially incident light, whereas the average cone catches only $\sim$23% of it. Thus, a typical red rod may be a fourfold better absorber of axial light than a single cone (at the λ_{max} of their respective visual pigments). However, the cone outer segment volume, V_c, as calculated previously, is nearly 100-fold smaller than that of the rod. The rod/cone ratio expected, 1, is similar to that assessed from published micrographs (means of 1–1.5; Kinney and Fisher, 1978a; Hollyfield et al., 1984; Röhlich and Szél, 2000). The fact that cones absorb a smaller portion of the incident light is not a handicap under daylight conditions, when high absolute sensitivity is not required. For the same reason, the loss of light by leakage from cone ellipsoids can be tolerated when light is plentiful. Therefore, frog rods and cones can serve the retina equally well despite their large disparity in size. By making cones with large entrance aperture and an ability to concentrate light, outer segment size reduction becomes possible at some cost in detector efficiency and sacrifice in acuity.

Upon review of the preceding examples, the data suggest a positive relationship between outer segment taper and ellipsoid concentration factor, F_C. The latter variable is a measure of light concentration from the ellipsoid into the outer segment. We have plotted the ratio $a_z'^{-1}/a_{h1}^{-1}$, indicating how many critical characteristic lengths would equal the characteristic length considered realistic, against F_C for the various species examined (Fig. 6, A and B). The correlations are positive,

though not particularly strong, especially when all the species studied are considered (Fig. 6 B). The lack of a strong correlation for the ensemble of species may in part reflect the lower accuracy of data obtained from histological material (especially from published figures) as opposed to live cell measurements. In addition, and perhaps more importantly, it may be an indication of other factors, such as the presence of oil droplets or light losses caused by ellipsoid leakage, affecting the extent of outer segment taper, none of which were considered in the calculations (for an instance of light loss estimation, see Baylor and Fettiplace, 1975). Nevertheless, the correlations, albeit approximate ones, between the cone ellipsoid concentration factor and outer segment taper expressed as a multiple of critical taper support the third function.

DISCUSSION

Emerging view on structure–function relations in vertebrate photoreceptors

Our analysis supports the three postulated functions for cone taper: (1) compensation for light loss resulting from self-screening, (2) increased signal-to-noise ratio along the length of the outer segment, and (3) improved light capture and material savings by shape continuity between inner and outer segment. Cone taper, as determined in this work, was found quite variable and, for the most part, beyond that predicted for critical taper (Table 2 and Fig. 3). Consequently, cones appear to achieve full compensation for the light loss caused by self-screening while improving signal-to-noise ratio along their outer segments. Support for the third function points to a dominant role of the inner segment in shaping the outer segment, leading to a process of miniaturization and, as a result, metabolic savings in biomaterials. The trade-offs in such structural modifications are in absolute sensitivity and visual acuity, with spatial resolution being inversely related to receptor cross section (Snyder and Miller, 1977; Neave, 1984; van der Meer, 1992; Haug et al., 2010). Large cone ellipsoids combined with excessively tapered outer segments could achieve miniaturization, but only in the presence of light funneling. Therefore, an ellipsoid light concentration property was suggested by logic and implied by the third function.

In every retinal region, a trade-off is expected between acuity and receptor size. The typical example is the retina of some diurnal teleosts where the highest visual acuity, found in the mid to upper frontal field, is subserved by smaller, densely packed cones in the centro- and ventro-temporal areas of the retina (Beaudet et al., 1997; Novales Flamarique, 2005, 2011; Cheng and Novales Flamarique, 2007). Other more extreme examples are the specialized foveas of diurnal lizards (Röll, 2001; Barbour et al., 2002) and primates (Borwein, 1981). In primates, high visual acuity is the product of tightly packed, long, rodlike foveal cone outer segments, each having a diameter of ∼1 µm; these are connected by cone fibers to the rest of their compartments that are laterally displaced and squeezed out to the slopes of the foveal pit (Borwein, 1981; Packer et al., 1989). Foveal cones have no ellipsoids, and, therefore, they must collect light without the aid of any other structure. However, parafoveal cones, and other cones in general, are built with joint outer and inner compartments, where the latter is the thicker of the two to intercept a larger area of retinal illumination at the cost of reduced regional acuity (Packer et al., 1989; Hoang et al., 2002). As flux is funneled from the entrance aperture to a smaller exit aperture at the distal end of ellipsoids, structural modifications become feasible in outer segment tapering and size. Cone miniaturization has several advantages, including improved signal-to-noise ratio, faster visual pigment regeneration (i.e., recovery from bleaching), and material savings as a result of reduced volume. The drawbacks are reduction in absolute sensitivity vis-à-vis rods and some light losses from detection as a result of ellipsoid leakage.

Rods, on the other hand, are specialized for high absolute sensitivity and not for rapid response (Burns and Lamb, 2003). The eyes of deep-sea fishes provide exquisite examples for such sensitive detector structures (Locket, 1977). The cylindrical form appears well suited for on-demand tailoring of outer segment length, which may reach hundreds of micrometers in fish species living at great depths. The use of multiple banks and assemblages of rods, in addition to long ones, also appears to be aimed at catching scarce photons in the darkness of the deep ocean (Locket, 1977; Munk, 1977; Collin et al., 1998). Rods do not jeopardize detection efficiency by the use of light-concentrating schemes at the ellipsoid level; they have wider acceptance angles for oblique rays than cones do. Other mechanisms, however, may operate to concentrate light onto the outer segment. For instance, some nocturnal mammals, like the mouse, show an inverted chromatin nuclear pattern that, together with a quasi-columnar organization of rod nuclei, serves to channel light from the outer nuclear layer toward the outer segments (Solovei et al., 2009). Signal pooling from multiple rods (at a sacrifice of spatial resolution) and coincidence detection should further improve scotopic performance as well as signal-to-noise ratio (Peichl, 2005).

Improved light funneling by oil droplets

Oil droplets are optical devices used by most cones in avian, amphibian, and reptilian eyes. Oil droplets are highly refractive spherical globules (Ives et al., 1983); they may be clear or colored (Kolb and Jones, 1987; Hart et al., 2006). Because of their location at the distal

end of inner segments anterior to the base of outer segments, they may serve as light filters as well as focusing devices (Young and Martin, 1984; Vorobyev, 2003). A spherical body with high refractive index immersed in a lower index medium will behave as a positive lens with a short focal length. Thus, an oil droplet (or a concentrated group of microdroplets, as in diurnal snakes; Wong, 1989) is expected to further concentrate the light funneled by the ellipsoid. As such, increased outer segment tapering and size reduction become feasible. And indeed, observational evidence bears this out: the most extreme cases of outer segment volume reduction are found in oil droplet–containing cones (Fig. 1). Oil droplet focusing might be advantageous not only in allowing further reductions in detector cross section, but also in quickening recovery from blinding exposures, as when experiencing glare.

For an elaboration of the last point, note the following: whereas scotopic sensitivity in primate and teleost vision may take tens of minutes to regain dark-adapted levels after a bright "bleaching" exposure, photopic sensitivity returns to former levels in a few minutes (Rushton, 1965; Thomas and Lamb, 1999; Kenkre et al., 2005; and unpublished data for teleosts). This indicates that cones recover their sensitivity in vivo faster than rods do. Experiments in vitro also reveal the same tendency in chemical regeneration of visual pigment: in the presence of copious amounts of exogenous 11-cis retinal, whereas rods regenerate slowly, cones recover rapidly and repeatedly after several bleaching exposures, and, in each case, they regain most of their visual pigment in a few seconds (Hárosi, 1984). Consider now the oil droplet–equipped cones in a fishing bird's eye. Given the short focal lengths of spherical lenses, an oil droplet will focus light in a specific region of an outer segment lamella, which would receive intense illumination. Let's assume, for the sake of the argument, that only 10% of a lamella is illuminated. When the bird skims over a body of water, reflected sunlight could be a blinding experience. In case of a human observer, extensive bleaching in retinal receptors would occur, resulting in temporary blindness. However, in cones with oil droplet focusing, only a fraction of the visual pigment complement would get bleached, and, in the assumed lamella, 90% of the visual pigment would remain unexposed. Because lateral and rotational diffusion drives visual pigment molecules rapidly in the receptor membranes (Wang et al., 2008), the bleached molecules would quickly be exchanged with unbleached ones from the adjacent membrane area. Therefore, most of the cone's sensitivity could recover in milliseconds, at least three orders of magnitude faster than a recovery based on normal biochemical regeneration (Kenkre et al., 2005).

The aforementioned mechanism could improve the foraging performance of birds like the black phoebe, a sit-and-wait predator whose visual searching increases significantly under bright light conditions, likely as a result of the negative effects of glare (Gall and Fernández-Juricic, 2009). Other bird species like herons and osprey routinely hunt in shady habitat or at crepuscular periods (unpublished data), reducing their exposure to glare and other blinding factors such as the light flickers produced by waves near the water surface. In fact, such flicker may be used by fish for camouflage, as multiple species have developed body markings that resemble the light patterns (McFarland and Loew, 1983). Fast-moving predators, like some insects and birds, have critical fusion frequencies that surpass the predominant flicker occurring in surface waters (in the range of 1–5 Hz), improving visual contrast of underwater targets (McFarland and Loew, 1983). Given a mean diffusion coefficient of 0.4 $\mu m^2 s^{-1}$ for activated opsins (Wang et al., 2008), between ~3 and 13% of the (bleached) visual pigment molecules in a 1-μm-diameter lamellae would get replaced by intact ones between flickers, contributing to fast recovery from bleaching.

On light collection mechanisms

The idea that cone inner segments concentrate light has been around for a long time. For instance, O'Brien (1946) proposed it in his theory explaining the Stiles-Crawford effect (O'Brien, 1951; Johnson and Tansley, 1956; Enoch, 1963). Concerning vertebrate photoreceptors, turtle cone ellipsoids have been compared with ideal light collectors (Baylor and Fettiplace, 1975; Winston, 1981). The name refers to nonimaging optical devices that concentrate light by internal reflection onto the smallest possible exit aperture (Winston, 1970). In the case of an invertebrate eye, Levi-Setti et al. (1975) suggested that the crystalline cone in an ommatidium of *Limulus* is an ideal light collector. Subsequent work by Land (1979), however, showed that the crystalline cones can form images and that they pass light through a refractive index variation scheme. Similar refractive index gradients have not been uncovered in vertebrate photoreceptors, and the mechanism of importance remains to be sorted out. Internal reflection, refraction, and even diffraction may play some role. Cone ellipsoids are not truly homogeneous, as they contain abundant mitochondria that might function akin to a Fresnel zone plate. The one conclusion that is certain at present is that an oil droplet must have a major contribution to the refractive power of the system. Another open question is whether investigations of waveguide modal patterns in vertebrate visual cells would facilitate the understanding of structure–function relationships between photoreceptor compartments (Snyder and Menzel, 1975).

Oblique incidence and the Stiles-Crawford effect

Stiles and Crawford (1933) discovered that the visual sensitivity of the human eye depends on the direction from which light enters the pupil (known as the Stiles-Crawford

effect of the first kind [SCE_1]). O'Brien (1946) was the first to advance a theory to explain it, and there have been others (e.g., Snyder and Pask, 1973; reviewed by Enoch and Bedell, 1981). The third hypothesis is consistent with the SCE_1. Accordingly, cone ellipsoids are imperfect concentrators; they lose light by leakage. The lower refractive indices of cone inner and outer segments provide reduced critical angles as compared with those of rods (Appendix 1). But rods, with more uniform and denser distal compartments, have larger critical angles and thus can tolerate a wider range of off-axis rays. The combination of these properties may be sufficient to account, at least qualitatively, for the larger photopic and smaller scotopic SCE_1 (Enoch and Bedell, 1981). Further support for the third function comes from a finding by Westheimer (1967) that foveal cones of the human eye have a reduced (i.e., rodlike) Stiles-Crawford effect when compared with parafoveal cones. Also supportive is the small directional sensitivity displayed by the human achromat, an abnormal condition in which vision depends entirely on rod function (Nordby and Sharpe, 1988).

Summary

We have provided evidence to support the notion that cone outer segment taper follows from the shape of the ellipsoid, a structure that serves to concentrate light onto the outer segment. The advantages of taper and cone miniaturization include compensation for light loss caused by self-screening, metabolic savings in structural components, higher signal-to-noise ratio, and accelerated regeneration of visual pigment. The trade-offs are in absolute sensitivity and visual acuity. As suggested by the different sizes of photoreceptors and their relative densities across phylogenetic groups, species have evolved visual cells that presumably optimize these trade-offs for life in particular environments. As such, there is no model cone or rod but a range of sizes and shapes dictated by the ecological constraints guiding the evolution of each species.

APPENDIX 1

Derivation of equations to test the first biophysical function: Cone outer segments taper to compensate for light flux diminution by absorption (self-screening) so that flux density remains invariant or increases with axial distance along the outer segment

The list of symbols and definitions used in the testing of this function are shown in Table 3. The following sections present geometric and spectrophotometric definitions of key variables (e.g., absorption coefficient and taper) used to evaluate whether a cone taper is critical, i.e., whether it compensates exactly for light flux diminution by self-screening (Hodgkin and O'Bryan, 1977). As a consequence, taper that is equal to or exceeds the critical value indicates compensation for self-screening.

Geometric derivation of the absorption coefficient

Perfect compensation for light absorption caused by self-screening imposes two requirements. The first is invariance of flux density with respect to z, so that $J_o = J_z$; in other words, the light flux impinging on the base (Φ_o) divided by the cross-sectional area (A_o) is equal to the transmitted flux (Φ_z) divided by the corresponding cross section (A_z) along the entire length of the outer segment. Accordingly,

$$\Phi_o/A_o = \Phi_z/A_z. \tag{1}$$

The second requirement is that visual pigment absorption be the only reason for the diminution of flux (i.e., light leakage is absent). This means that the incident light rays interact with the cell boundary at angles (Θ) below the critical angle (Θ_c) so that total internal reflection prevents light from escaping (see the section Critical angle estimations for data confirming this). Thus,

$$\Theta \le \Theta_c. \tag{2}$$

The exponential law of absorption,

$$\Phi_z = \Phi_o \exp(-az), \tag{3}$$

sets forth the variation of flux in an absorbing medium along the z direction (Φ_z) in terms of the incident flux (Φ_o) multiplied by an exponential function of variable (z) and a characteristic constant of the medium, called the absorption coefficient (a). The latter is inversely proportional to the attenuation, or characteristic, length, at which Φ falls to $\exp(-1) = 0.368$ of Φ_o. Upon combining Eqs. 1 and 3, we obtain

$$\Phi_z/\Phi_o = A_z/A_o = \exp(-az). \tag{4}$$

The circular cross section of a cone with diameter d is $A = d^2\pi/4$, and thus, Eq. 4 may be written as

$$d_z = d_o \exp(-az/2), \tag{5}$$

wherefrom the absorption coefficient for testing the first function is expressible as

$$a_{h1} = (2/z)\ln(d_o/d_z). \tag{6}$$

The surprising outcome gleaned from Eq. 6 is that the absorption coefficient, a purely spectroscopic quantity, may be determined from measurements of distance involving the base diameter, d_o, a second diameter, d_z, and their separation along the z coordinate.

TABLE 3

List of symbols and definitions pertaining to the first biophysical function

Symbol	Definition
Φ	Total light flux (photons s^{-1})
Φ_o, Φ_z	Value of Φ at z = 0 and at distance z from base
A	Cross-sectional area of outer segment, assumed to be equal with the surface area of a transverse membrane, referred to as a lamella (Eckmiller, 1987). One rod disk, also called flattened saccule, has the surface of two lamellae
A_o, A_z	Value of A at the base and at distance z from it
$A_\perp$, $A_\parallel$	Outer segment absorbance for transversely and axially polarized light
J_o	Incident flux density (photons s^{-1} μm^{-2}); $J_o = \Phi_o/A_o$
J_z	Transmitted flux density through level z from base; $J_z = \Phi_z/A_z$
R	Dichroic ratio: absorbance ratio at two orthogonal polarizations; $R = A_\perp/A_\parallel$
$S_\perp$	Specific absorbance at transverse polarization; $S_\perp = A_\perp/d$
d	Outer segment diameter (mean)
d_o, d_z	Outer segment diameter at base and at a distance z from the base
c	Concentration of visual pigment in appropriate units
α	Molecular extinction coefficient (μm^2 per molecule; Eqs. 7 and 9)
ε	Molar extinction coefficient (liter $mole^{-1}$ cm^{-1}; Eqs. 8 and 9)
λ_{max}	Wavelength of peak extinction
k	Anisotropy factor: ratio of anisotropic to isotropic absorbance
a	Absorption coefficient (usually in cm^{-1}; Eq. 3)
a^{-1}	Characteristic length (reciprocal of a) expressed in μm (signifies the distance at which Φ_z reduces to 36.8% of Φ_o)
a_{h1}	Absorption coefficient required for invariance of light flux along the outer segment, as by Eq. 6
$a_{h1}{}^{-1}$	Characteristic length, based on invariance of light flux along an outer segment (μm)
a_z'	Absorption coefficient obtained by Eq. 10
a_z''	Absorption coefficient obtained by Eq. 16
$a_z'^{-1}$, $a_z''^{-1}$	Characteristic lengths (μm) obtained from a_z' and a_z''
τ	Taper, as defined by Eq. 17
Θ	Angle of incidence with respect to cell axis
Θ_c	Critical angle of Θ, defined as $\Theta_c = 90° - \varphi_c$
φ_c	Critical angle with respect to normal of boundary (Eq. 19)
φ_i, φ_o	Angles of incidence and refraction to normal of boundary
n_1, n_2	Refractive indices of two optical media forming a boundary
z	Axial distance within outer segments (μm), with z = 0 at the base

Spectrophotometric determinations of the absorption coefficient

Two methods have been established for the determination of the axial absorption coefficient of a vertebrate photoreceptor outer segment in situ (Hárosi and MacNichol, 1974; Hárosi, 1975, 1982). The first one requires knowledge of the visual pigment's molar extinction coefficient, ε, its equivalent (random) molar concentration, c, and the dichroic ratio, R, or some equivalent measure of anisotropy. The second method makes use of the transverse specific absorbance, $S_\perp$, determined in a side-on oriented outer segment. The two methods are interdependent by the dichroic ratio, R, as shown in the section Anisotropic absorbance by visual cells.

Isotropic absorbance by solutions

The light-absorbing property of a homogeneous, isotropic medium is expressed in terms of either the natural or the decadic logarithm of incident to transmitted light fluxes. Thus, absorbance (optical density) may be written as

$$D_1 = \ln(\Phi_o/\Phi_z) = \alpha c z \tag{7}$$

$$\text{or } D_2 = \log(\Phi_o/\Phi_z) = \varepsilon c z, \tag{8}$$

in which c is the concentration, z is the path length, and α is the molecular or chromophoric (Napierian) and ε is the molar (decadic) extinction coefficient of the light-absorbing substance. Substituting Eq. 3 in Eqs. 7 and 8, the absorption coefficient for a random ensemble of absorbing molecules can be related to α and ε as

$$a = \alpha c = 2.303\, \varepsilon c. \tag{9}$$

Note that a, α, and ε are applicable to isotropic pigments and that they are also wavelength dependent. Their values at λ_{max} are often used as single-valued parameters (e.g., Warrant and Nilsson, 1998).

Anisotropic absorbance by visual cells

Rod and cone outer segments in side view exhibit intrinsic linear dichroism, revealing their anisotropic nature. Because the absorption vectors of the visual pigment molecules lie nearly parallel with the lamellar (x-y) planes, axially traveling light (z direction) is well absorbed; this makes photoreceptors more effective light catchers in this direction than an isotropic solution of the same pigment would be at the same concentration and path length.

By a generalization of Eq. 9, the first formula to express the end-on (axial) absorption coefficient along the z direction is

$$a_z' = k\alpha c = 2.303\, k\varepsilon c, \tag{10}$$

in which k is the anisotropy factor accounting for the gain by the ordered distribution; k may be as large as 1.5 (perfect two-dimensional random array) and as small as 1.0 (three-dimensional random array). By polarized absorbance measurements of side-on oriented receptors, the dichroic ratio, defined as $R = A_\perp/A_\parallel$, can be determined, and k can be expressed as a function of R, as follows.

If a cylindrical vessel is homogeneously filled with N absorbing molecules, each possessing a transition moment M, the total extinction (E = NM) may be written as $E = E_x + E_y + E_z$. The fractions expressed in the three spatial coordinates are equal for a three-dimensional random array so that $E_x/E = E_y/E = E_z/E = 1/3$. The measurable fraction of extinction in the z direction is half of the two orthogonal components:

$$0.5\left(E_x + E_y\right)/E = 1/3. \tag{11}$$

In a similar model, a cylindrical photoreceptor may be regarded, in its simplest form, as an imperfect two-dimensional random array for which $E_x = E_y$ and $E_x/E_z = R$. With these, the z fraction is expressible as

$$E_z/E = E_z/\left(2E_x + E_z\right) = 1/\left(1 + 2R\right). \tag{12}$$

Viewed from the z direction (i.e., end-on), the measurable fraction is

$$\begin{aligned} &0.5\left(E_x + E_y\right)/E = 0.5\left(E - E_z\right)/E = \\ &0.5\left[1 - 1/\left(1 + 2R\right)\right] = R/\left(1 + 2R\right). \end{aligned} \tag{13}$$

The anisotropy factor (k) in the z direction is obtainable from the above as the ratio of end-on extinctions (the two-dimensional versus the three-dimensional fractions) and is given by (see Hárosi, 1975, 1982)

$$k = 3R/\left(1 + 2R\right). \tag{14}$$

Thus, ε, c, and R yield the axial absorption coefficient of a photoreceptor with the aid of Eqs. 10 and 14.

The second formula for the calculation of the axial absorption coefficient makes use of the microspectrophotometrically determined transverse specific absorbance, $S_\perp = A_\perp/d$, in which $A_\perp$ is the peak absorbance (of the α band) for transversely polarized light of the outer segment in side-on orientation and d is the mean cell diameter, presumed to be equal with transverse path length. The following relationship,

$$(\varepsilon c) = S_\perp\left(1 + 2R\right)/3R, \tag{15}$$

has been found useful in relating in vitro spectrophotometric data to those obtained by in situ microspectrophotometry (Hárosi, 1975). The substitution of Eqs. 14 and 15 into Eq. 10 leads to the desired equation:

$$a_z'' = 2.303\, S_\perp. \tag{16}$$

Therefore, the axial absorption coefficient is also attainable from the transverse specific absorbance by Eq. 16. Anisotropy is implicit in $S_\perp$ since Eq. 15 may also be written as $S_\perp = k(\varepsilon c)$. The latter relationship shows the interdependence of Eqs. 10 and 16, which, therefore, lead to dependent estimates of the axial absorption coefficient, even though the two are based on different determinations.

A definition of taper

As a geometrical characterization of a cone taper, τ is defined here as the angle between the axis and the inclination of the contour line, which, upon precession, describes the conical surface:

$$\tau = \tan^{-1}[(d_o - d_z)/2z]. \tag{17}$$

The axial distance, z, is the separation between the base of a right cone, with diameter d_o, and a parallel slice, with diameter d_z. For a cone cell, τ describes an average inclination of the contour line between two slices (corresponding to d_o and d_z), and it cannot account for a point-by-point variation that Eq. 5 describes.

Critical angle estimations

The refractive indices for rod and cone inner and outer segments have been measured only for a few animal species in a handful of studies. The obtained values are as follows: the refractive index for rod ellipsoid and outer segment, 1.40 and 1.41, respectively; for cone ellipsoid and outer segment, 1.39 and 1.385, respectively; and for the extracellular matrix (mucopolysaccharide), 1.34 (see Borwein, 1981 for primary citations).

At a boundary between two transparent media, one denser with refractive index n_1 (inside), the other rarer with refractive index n_2 (outside), light rays will refract according to Snell's law:

$$n_1 \sin\varphi_i = n_2 \sin\varphi_o, \tag{18}$$

in which φ_i and φ_o are the corresponding angles of incidence and refraction with respect to the normal. Beyond a certain angle of incidence in the denser medium, no refraction occurs, and there is total internal reflection. The critical angle (for which $\sin\varphi_o = 1$) can be expressed from Eq. 18 as

$$\varphi_c = \sin^{-1}\left(n_2/n_1\right). \tag{19}$$

From this, Θ_c of Eq. 2 can now be obtained as

$$\Theta_c = 90° - \varphi_c. \tag{20}$$

Substitution of the numerical values cited above in Eqs. 19 and 20 leads to the following critical angles in Θ_c: 15.4° and 14.6° for cone ellipsoid and outer segment and 16.8° and 18.1° for rod ellipsoid and outer segment, respectively. In these calculations, we assumed that the relevant optical parameters used in critical angle calculations are those that have been determined (Borwein, 1981), notwithstanding the fact that photoreceptors and their surroundings are neither homogeneous nor isotropic.

TABLE 4

Additional list of symbols and definitions pertaining to the second biophysical function

Symbol	Definition
Φ_a, Φ_{az}	Absorbed flux in one layer at the base and at depth z
J_n	Surface density of pigment (molecules μm^{-2}); $J_n = n/A_t$
δ	In situ path length in visual cells corresponding to a single pigment-laden lipid bilayer (lamella); δ = 15 nm is taken as its equivalent thickness
A_t	Total lamellar surface area of an outer segment
c	Concentration of visual pigment; $c = n/A_t\delta = J_n/\delta$
n	Total number of visual pigment molecules contained in an outer segment
n_o, n_z	Number of visual pigment molecules in a lamella at the base and at z
p_z	Probability of absorption of a quantum by a single layer at z
γ	Quantum efficiency of bleaching; number of photons absorbed per number of photoactivations that result in bleaching
S_z	Signal from light activation (ionic current) at level z
N_z	Noise produced in the dark at level z (ionic current)

What constitutes the surrounding medium is especially questionable. This, sometimes referred to as interstitial matrix, is commonly equated with mucopolysaccharide, as done here. However, microvilli of the pigmented epithelial cells and the calycal processes that come in contact with at least parts of inner and outer segments may play a role in setting the refractive properties of these cells.

Outer segment taper, as defined by Eq. 17 and determined from our observations and published photomicrographs (see Results), indicate angles <14°. These values are within the requirement of Eq. 2, and thus, they justify the original assumption concerning the funneling of axial rays by total internal reflection.

APPENDIX 2

Derivation of equations to test the second biophysical function: Cone outer segments taper to improve signal-to-noise ratio along their lengths

The list of symbols and definitions used to evaluate this function are presented in Table 4. We make the following five assumptions. (1) Incident light consists of an axial flux of parallel, uniform, and steady illumination at the base of outer segments with negligible reflection and scattering losses. (2) Visual pigment molecules are packed uniformly in transverse membranes of all rods and cones with constant surface density: $J_n = n/A_t = n_o/A_o = n_z/A_z$. (3) Activation of visual pigment molecules requires not only light absorption but also chromophore isomerization, commonly referred to as bleaching. To take this into account, the quantum efficiency of bleaching, γ, must be factored in (Dartnall et al., 1936). (4) Signal is constituted by a photocurrent generated through the cell envelope at each lamella, independent of other lamellae. Although there clearly is an observable spreading of excitation, for the sake of simplicity, all messengers for signal are assumed to originate in one lamella. (5) Noise is generated like signal in lamellae under the conditions set forth in the preceding assumption. Whether thermal isomerization of the chromophore or subsequent biochemical steps are the cause (Rieke and Baylor 1996, 2000; Sampath and Baylor, 2002; Holcman and Korenbrot, 2005), it is assumed here that noise is proportional to the number of visual pigment molecules contained within each layer.

The objective of this appendix is to relate the generation of signal and noise to outer segment taper. Given an absorbing medium, an incident flux will either be absorbed or transmitted, provided that assumption 1 holds. In general terms,

$$\Phi_o = \Phi_a + \Phi_z. \tag{21}$$

When normalized to the incident flux, Eq. 21 may be rearranged as

$$\Phi_a/\Phi_o = 1 - \Phi_z/\Phi_o. \tag{22}$$

The left-hand side in Eq. 22 is usually referred to as absorptance, $A_b = \Phi_a/\Phi_o$, whereas the fraction on the right-hand side is called transmittance, $T = \Phi_z/\Phi_o$. Optical density (or absorbance), as defined previously in Eq. 7, is the logarithm of T^{-1}. After substitution of Eq. 3 in Eq. 22 and rearrangement, the rate of photon absorption by a monolayer of thickness δ, with incident flux Φ_o, is

$$\Phi_a = \Phi_o[1 - \exp(-a\delta)]. \tag{23}$$

Because visual pigments are hydrophobic chromoproteins, they must be membrane bound. For this reason, the shortest meaningful axial path length of the visual pigment in a vertebrate photoreceptor is a single layer. Although the exact numerical value of δ for the present is immaterial, it is assumed to be 15 nm. This is half the repeat distance of the 30 nm obtained for rod disks by electron microscopic and x-ray crystallographic determinations (for references, see Fein and Szuts, 1982). The value of $\delta = 1.5 \times 10^{-6}$ cm permits estimation of the magnitude of the exponent in Eq. 23. Based on Eqs. 10 and 14, the absorption coefficient for a "typical" rhodopsin-containing cone is expected to be near 420 cm^{-1} (a^{-1} = 24 μm), which would make the value of the exponent $\sim 6.3 \times 10^{-4}$.

In view of the probable magnitude of δ and assumption 2, and also considering pigment anisotropy according to Eq. 10 and expressing the concentration as

$$c = n/A_t\delta = J_n/\delta = n_z/A_z\delta, \tag{24}$$

we can derive the following formula from Eq. 23:

$$\Phi_a = \Phi_o[1 - (1 - k\alpha c\delta)] = \Phi_o k\alpha n_z/A_z, \tag{25}$$

in which the exponential term in Eq. 23 was represented by the first two terms of its series expansion (the second and higher order terms being negligibly small). Thus, the rate of absorption in a pigment layer is proportional to the incident light flux times the products of anisotropy factor (k), pigment type (α), and surface density of the pigment ($J_n = n_z/A_z$). By extending Eq. 25 to describe a multilayered system with self-screening, the rate of absorption by one layer at depth z is

$$\Phi_{az} = k\alpha\left(n_z/A_z\right)\Phi_o\exp\left(-az\right). \tag{26}$$

A second method of obtaining the rate of quantum absorption by a single layer of visual pigment is based on the interpretation of the chromophoric absorption coefficient (α) as the absorption cross section of one molecule in a random array (Dartnall, 1972). The probability of a quantum at λ_{max} to be caught by a single layer of visual pigment, with anisotropy factor k, is expressible as a ratio of the sum of all the molecular cross sections to that of the available total area:

$$p_z = k\alpha n_z/A_z. \tag{27}$$

When we scale up from one photon to an incident photon flux of Φ_o, Eq. 27 will reproduce the preceding relationship described by Eq. 25.

The rate of signal generation in a lamella at z is expected to be proportional to the rate of photon absorption in that layer (assumptions 3 and 4). Thus, the signal should be formally similar to Eq. 26:

$$S_z = C_S k\alpha\gamma\left(n_z/A_z\right)\Phi_o\exp\left(-az\right), \tag{28}$$

with C_S being a conversion factor between photon absorption and corresponding photocurrent.

The noise produced at layer z may be given (assumption 5) as

$$N_z = C_N n_z, \tag{29}$$

in which C_N is again a conversion factor. In taking the ratio between Eqs. 28 and 29, n_z will cancel out, and the signal-to-noise ratio becomes (with C′ as a new constant)

$$S_z/N_z = C'k\alpha\gamma(\Phi_o/A_z)\left[\exp\left(-az\right)\right]. \tag{30}$$

APPENDIX 3

Derivation of equations to test the third biophysical function: Cone outer segments taper in accordance with the optical properties of their inner segments, facilitating light capture and reducing use of biomaterials

The list of symbols and definitions used to evaluate this function are presented in Table 5. The following sections introduce definitions of key variables (e.g., concentration factor) for its evaluation.

Assuming a perfect two-dimensional random array of absorbers, the angle of incidence with respect to the optic axis (Θ) will reduce the absorption probability of unpolarized light by a factor (Winston, 1981):

$$f = 0.5\,(1 + \cos^2\Theta). \tag{31}$$

Evaluated for Θ = 15°, Eq. 31 yields f = 0.97. Thus, oblique incidence for angles up to 15° causes only a small drop (3%) in absorption efficiency. In the following treatment, we assume, therefore, that oblique incidence does not significantly affect the in situ absorption efficiency of the visual pigment molecules embedded in the transverse lamellae.

Flux concentration in a tapered outer segment

In the absence of absorption, the flux density of a converging (conical) beam increases in the direction of convergence. The conceptually simplest case occurs when the incident cone of light matches exactly the outer segment taper. This, however, leads to the same analysis covered previously, where an axially parallel beam was assumed to be incident on the base of a tapered outer segment, in which total internal reflection prevailed. In terms of flux densities, Eq. 26 may also be written as

$$J_{az} = J_o\left(A_o/A_z\right)k\alpha\left(n_z/A_z\right)\exp\left(-az\right) \tag{32}$$

to indicate a rate of absorption density increase by the factor A_o/A_z. For obtaining the signal generation in a lamella at z, however, the total absorbed flux is needed, not the flux density. Multiplying Eq. 32 by A_z, though, takes us back to Eq. 26. Therefore, the preceding analysis leading to Eq. 30 is also valid for this case.

Besides the matching case, the convergence of the beam incident upon the outer segment may also be lesser or greater than that of the structure. The slightly convergent case is the simplest one, and it may be handled as the axially parallel beam was above (see previous paragraph), necessitating no new analysis. The greater beam convergence, however, warrants further considerations. Some aspects of the latter case are discussed in the manuscript in connection with the effect of oil droplet focusing.

Flux concentration in a cone ellipsoid

The third function presupposes the existence of a mechanism whereby cone ellipsoids funnel light from a broader, proximal portion toward a narrower, distal end and that this property makes a significant impact on the structure and function of outer segments. Consider a flux Φ_i incident at the entrance aperture (largest cross section) of an ellipsoid to produce a flux density J_i. If this flux is coupled without loss to a smaller exit aperture,

TABLE 5

Additional list of symbols and definitions pertaining to the third biophysical function

Symbol	Definition
f	Absorption efficiency factor due to oblique incidence (Eq. 31)
A_i	Collection area (circular); largest cross section of inner segment
d_i	Diameter of A_i
Φ_i	Total flux at entrance aperture of an inner segment
J_i	Flux density at entrance aperture of an inner segment
J_{az}	Rate of flux density absorption
F_C	Concentration factor (Eq. 33)
F_G	Geometry factor (Eq. 35)
d_t	Diameter at the tip of a frustum
h	Altitude or height of a cone or cylinder
V_r	Volume of a rod outer segment
V_c	Volume of a cone outer segment
V_{req}	Volume of an optically equivalent rod outer segment
V_R	Volume reduction ratio as defined by Eq. 36

where the flux density is J_o, the following relationships hold (provided the cross sections are circular with respective areas and diameters of A_i, d_i and A_o, d_o):

$$J_o/J_i = A_i/A_o = \left(d_i/d_o\right)^2 = F_C. \quad (33)$$

The significance of F_C, named here concentration factor, is that it shows the proportion by which the base of a photoreceptor can be reduced in area while still capable of detecting all of the incident flux Φ_i. Although the issue of light losses by leakage remains to be considered, this property reveals the feasibility of detector miniaturization.

Volume reduction of a cone outer segment

Whereas the outer limb of rods approaches the cylindrical form in nearly all instances, cone outer segments usually appear truncated, not pointed. Therefore, the frustum of a cone is a more realistic representation of a cone outer segment. The volume of the frustum of a cone is defined with a diameter of base d_o, of tip d_t, and altitude h as

$$V_c = (\pi/4)(h/3)\left[d_o^2 + d_o d_t + d_t^2\right]. \quad (34)$$

Compared with the volume of a cylindrical rod, $V_r = (\pi/4)hd_o^2$, their ratio is defined as

$$V_r/V_c = F_G, \quad (35)$$

in which F_G is named the geometry factor. Experience shows that the value of F_G is variable and tends to fall between 1.5 and 3, the latter being the largest for a right cone ($d_t = 0$). With these two factors combined, the volume reduction ratio is defined as

$$V_R = V_{req}/V_c = F_G F_C. \quad (36)$$

V_R is an indicator of proportion between the outer limb volumes of a cone and an equivalent rod, when both have equal inner segment entrance aperture and incident flux. Discounting light losses, these two cells could produce the excitation of an equal number of visual pigment molecules to equal illumination. Clearly, the cone is the more efficient receptor of the two because it uses only a fraction of the rod's detector apparatus. This means reduced amounts in lipid membrane, visual pigment, and all the other components of the enzymatic cascade required for generating signals in terms of photocurrent modulation.

Dr. Ferenc I. Hárosi passed away in November 2008. During his career, he was the leading innovator in the field of microspectrophotometry, starting with the making of the first computerized dichroic microspectrophotometer in the 1970s. His insights into photoreceptor physiology and visual pigment properties opened new fields of investigation that are actively pursued by many a prominent scientist today. He was my friend and mentor and an inspiration to vision scientists of all ages. Dr. Hárosi is, and will always be, profoundly missed; thank you for everything, friend.

We are grateful to Drs. Gregor J. Jones, Edward F. MacNichol Jr., and Ete Z. Szuts for critical reading and helpful comments on earlier versions of the manuscript and to Dr. Juan Korenbrot for stimulating discussions on the subject. We also thank Dr. Catherine Carr, Ed Enos, and Mike Juhas for specimens or tissue used in the study and Lisa Grebinsky for logistical help.

This work was funded by the Natural Sciences and Engineering Research Council of Canada Discovery Grant 238886 and a Grass-Marine Biological Laboratory Sabbatical Fellowship in Neurosciences to I. Novales Flamarique.

Edward N. Pugh Jr. served as editor.

Submitted: 20 July 2011
Accepted: 21 December 2011

REFERENCES

Ahlbert, I.B. 1973. Ontogeny of double cones in the retina of perch fry (*Perca fluviatilis*, Teleostei). *Acta Zoologica (Stockholm, Sweden).* 54:241–254. http://dx.doi.org/10.1111/j.1463-6395.1973.tb00460.x

Ali, M.A., and M. Anctil. 1973. Retina of the South American lungfish, *Lepidosiren paradoxa* Fitzinger. *Can. J. Zool.* 51:969–972. http://dx.doi.org/10.1139/z73-140

Ali, M.A., and M. Anctil. 1974. Letter: Retinas of the electric ray (*Narcine brasiliensis*) and the freshwater stingray (*Paratrygon motoro*). *Vision Res.* 14:587–588. http://dx.doi.org/10.1016/0042-6989(74)90048-0

Ali, M.A., and M. Anctil. 1976. Retinas of Fishes: An Atlas. Springer-Verlag, New York. 248 pp.

Ali, M.A., and M. Anctil. 1977. Retinal structure and function in the walleye (*Stizostedion vitreum vitreum*) and sauger (*S. canadense*). *Journal of the Fisheries Research Board of Canada.* 34:1467–1474. http://dx.doi.org/10.1139/f77-211

Ali, M.A., M.A. Klyne, E.H. Park, and S.H. Lee. 1989. Structure of the external retina of the oviparous, hermaphroditic fish *Rivulus marmoratus* Poey. *Anat. Anz.* 168:7–15.

Anctil, M., and M.A. Ali. 1976. Cone droplets of mitochondrial origin in the retina of *Fundulus heteroclitus* (Pisces: Cyprinodontidae). *Zoomorphology.* 84:103–111. http://dx.doi.org/10.1007/BF02568559

Anderson, D.H., and S.K. Fisher. 1976. The photoreceptors of diurnal squirrels: outer segment structure, disc shedding, and protein renewal. *J. Ultrastruct. Res.* 55:119–141. http://dx.doi.org/10.1016/S0022-5320(76)80087-1

Araki, M., K. Watanabe, and K. Yasuda. 1984. Immunocytochemical localization of rhodopsin-like immunoreactivity in the outer segments of the rods and single cones of chick retina. *Cell Struct. Funct.* 9:1–12. http://dx.doi.org/10.1247/csf.9.1

Armengol, J.A., F. Prada, and J.M. Génis-Gálvez. 1981. Oil droplets in the chameleon (*Chamaeleo chamaeleo*) retina. *Acta Anat. (Basel).* 110:35–39. http://dx.doi.org/10.1159/000145410

Arrese, C.A., N.S. Hart, N. Thomas, L.D. Beazley, and J. Shand. 2002. Trichromacy in Australian marsupials. *Curr. Biol.* 12:657–660. http://dx.doi.org/10.1016/S0960-9822(02)00772-8

Arrese, C.A., J. Rodger, L.D. Beazley, and J. Shand. 2003. Topographies of retinal cone photoreceptors in two Australian marsupials. *Vis. Neurosci.* 20:307–311. http://dx.doi.org/10.1017/S0952523803203096

Arrese, C.A., A.Y. Oddy, P.B. Runham, N.S. Hart, J. Shand, D.M. Hunt, and L.D. Beazley. 2005. Cone topography and spectral sensitivity in two potentially trichromatic marsupials, the quokka (*Setonix brachyurus*) and quenda (*Isoodon obesulus*). *Proc. Biol. Sci.* 272:791–796. http://dx.doi.org/10.1098/rspb.2004.3009

Bailes, H.J., S.R. Robinson, A.E.O. Trezise, and S.P. Collin. 2006. Morphology, characterization, and distribution of retinal photoreceptors in the Australian lungfish *Neoceratodus forsteri* (Krefft, 1870). *J. Comp. Neurol.* 494:381–397. http://dx.doi.org/10.1002/cne.20809

Barbour, H.R., M.A. Archer, N.S. Hart, N. Thomas, S.A. Dunlop, L.D. Beazley, and J. Shand. 2002. Retinal characteristics of the ornate dragon lizard, *Ctenophorus ornatus*. *J. Comp. Neurol.* 450:334–344. http://dx.doi.org/10.1002/cne.10308

Baylor, D.A. 1987. Photoreceptor signals and vision. Proctor lecture. *Invest. Ophthalmol. Vis. Sci.* 28:34–49.

Baylor, D.A., and R. Fettiplace. 1975. Light path and photon capture in turtle photoreceptors. *J. Physiol.* 248:433–464.

Beaudet, L., I. Novales Flamarique, and C.W. Hawryshyn. 1997. Cone photoreceptor topography in the retina of sexually mature Pacific salmonid fishes. *J. Comp. Neurol.* 383:49–59. http://dx.doi.org/10.1002/(SICI)1096-9861(19970623)383:1<49::AID-CNE4>3.0.CO;2-L

Bell, G. 2009. Selection: The Mechanism of Evolution. Oxford University Press, Oxford. 576 pp.

Bernstein, S.A., D.J. Breding, and S.K. Fisher. 1984. The influence of light on cone disk shedding in the lizard, *Sceloporus occidentalis*. *J. Cell Biol.* 99:379–389. http://dx.doi.org/10.1083/jcb.99.2.379

Borwein, B. 1981. The retinal receptor: a description. *In* Vertebrate Photoreceptor Optics. J.M. Enoch and F.L. Tobey Jr., editors. Vol. 23. Springer-Verlag, New York. 11–81.

Borwein, B., and M.J. Hollenberg. 1973. The photoreceptors of the "four-eyed" fish, *Anableps anableps* L. *Journal of Morphology.* 140:405–441. http://dx.doi.org/10.1002/jmor.1051400404

Borwein, B., D. Borwein, J. Medeiros, and J.W. McGowan. 1980. The ultrastructure of monkey foveal photoreceptors, with special reference to the structure, shape, size, and spacing of the foveal cones. *Am. J. Anat.* 159:125–146. http://dx.doi.org/10.1002/aja.1001590202

Bowmaker, J.K. 2008. Evolution of vertebrate visual pigments. *Vision Res.* 48:2022–2041. http://dx.doi.org/10.1016/j.visres.2008.03.025

Bozzanao, A., R. Murgia, S. Vallerga, J. Hirano, and S. Archer. 2001. The photoreceptor system in the retinae of two dogfishes, *Scyliorhinus canicula* and *Galeus melastomus*: possible relationship with depth distribution and predatory lifestyle. *Journal of Fish Biology.* 59:1258–1278. http://dx.doi.org/10.1111/j.1095-8649.2001.tb00190.x

Bozzano, A. 2004. Retinal specialisations in the dogfish *Centroscymnus coelolepis* from the Mediterranean deep-sea. *Scientia Marina.* 68 (Suppl. 3):185–195. http://dx.doi.org/10.3989/scimar.2004.68s3185

Braekevelt, C.R. 1982. Photoreceptor fine structure in the goldeye (*Hiodon alosoides*) (teleost). *Anat. Embryol. (Berl.).* 165:177–192. http://dx.doi.org/10.1007/BF00305476

Braekevelt, C.R. 1983a. Photoreceptor fine structure in the domestic ferret. *Anat. Anz.* 153:33–44.

Braekevelt, C.R. 1983b. Retinal photoreceptor fine structure in the domestic sheep. *Acta Anat. (Basel).* 116:265–275. http://dx.doi.org/10.1159/000145750

Braekevelt, C.R. 1984. Retinal fine structure in the European eel *Anguilla anguilla*. II. Photoreceptors of the glass eel stage. *Anat. Anz.* 157:233–243.

Braekevelt, C.R. 1985. Retinal fine structure in the European eel *Anguilla anguilla*. IV. Photoreceptors of the yellow eel stage. *Anat. Anz.* 158:23–32.

Braekevelt, C.R. 1987. Photoreceptor fine structure in the vervet monkey (*Cercopithecus aethiops*). *Histol. Histopathol.* 2:433–439.

Braekevelt, C.R. 1988a. Retinal fine structure in the European eel *Anguilla anguilla*. VI. Photoreceptors of the sexually immature silver eel stage. *Anat. Anz.* 166:23–31.

Braekevelt, C.R. 1988b. Retinal fine structure in the European eel *Anguilla anguilla*. VIII. Photoreceptors of the sexually mature silver eel stage. *Anat. Anz.* 167:1–10.

Braekevelt, C.R. 1990a. Photoreceptor fine structure in light- and dark-adaptation in the butterfly fish (*Pantodon buchholzi*). *Anat. Anz.* 171:351–358.

Braekevelt, C.R. 1990b. Retinal photoreceptor fine structure in the mallard duck (*Anas platyrhynchos*). *Histol. Histopathol.* 5:123–131.

Braekevelt, C.R. 1990c. Fine structure of the retinal photoreceptors of the domestic cat (*Felis catus*). *Anat. Histol. Embryol.* 19:67–76. http://dx.doi.org/10.1111/j.1439-0264.1990.tb00879.x

Braekevelt, C.R. 1990d. Fine structure of the retinal photoreceptors of the ranch mink *Mustela vison*. *Acta Anat. (Basel).* 138:254–260. http://dx.doi.org/10.1159/000146948

Braekevelt, C.R. 1992a. Photoreceptor fine structure in the southern fiddler ray (*Trygonorhina fasciata*). *Histol. Histopathol.* 7:283–290.

Braekevelt, C.R. 1992b. Retinal photoreceptor fine structure in the velvet cichlid (*Astronotus ocellatus*). *Anat. Embryol. (Berl.).* 186:363–370.

Braekevelt, C.R. 1992c. Retinal photoreceptor fine structure in the red-backed salamander (*Plethodon cinereus*). *Histol. Histopathol.* 7:463–470.

Braekevelt, C.R. 1993a. Fine structure of the retinal photoreceptors of the tiger salamander (*Ambystoma tigrinum*). *Histol. Histopathol.* 8:265–272.

Braekevelt, C.R. 1993b. Retinal photoreceptor fine structure in the red-tailed hawk (*Buteo jamaicensis*). *Anat. Histol. Embryol.* 22:222–232. http://dx.doi.org/10.1111/j.1439-0264.1993.tb00360.x

Braekevelt, C.R. 1993c. Fine structure of the retinal photoreceptors of the great horned owl (*Bubo virginianus*). *Histol. Histopathol.* 8:25–34.

Braekevelt, C.R. 1994a. Retinal photoreceptor fine structure in the short-tailed stingray (*Dasyatis brevicaudata*). *Histol. Histopathol.* 9:507–514.

Braekevelt, C.R. 1994b. Retinal photoreceptor fine structure in the American crow (*Corvus brachyrhynchos*). *Anat. Histol. Embryol.* 23:376–387. http://dx.doi.org/10.1111/j.1439-0264.1994.tb00488.x

Braekevelt, C.R. 1998. Fine structure of the retinal photoreceptors of the emu (*Dromaius novaehollandiae*). *Tissue Cell.* 30:137–148. http://dx.doi.org/10.1016/S0040-8166(98)80062-1

Braekevelt, C.R., and K.C. Richardson. 1996. Retinal photoreceptor fine structure in the Australian galah (*Eolophus roseicapillus*) (Aves). *Histol. Histopathol.* 11:555–564.

Braekevelt, C.R., S.A. Smith, and B.J. Smith. 1996. Fine structure of the retinal photoreceptors of the barred owl (*Strix varia*). *Histol. Histopathol.* 11:79–88.

Braekevelt, C.R., S.A. Smith, and B.J. Smith. 1998. Photoreceptor fine structure in *Oreochromis niloticus* L. (Cichlidae; Teleostei) in light- and dark-adaptation. *Anat. Rec.* 252:453–461. http://dx.doi.org/10.1002/(SICI)1097-0185(199811)252:3<453::AID-AR13>3.0.CO;2-3

Brindley, G.S. 1970. Physiology of the retina and visual pathway. Second edition. Edward Arnold, London. 315 pp.

Bunt, A.H., and I.B. Klock. 1980. Fine structure and radioautography of retinal cone outer segments in goldfish and carp. *Invest. Ophthalmol. Vis. Sci.* 19:707–719.

Burns, M.E., and T.D. Lamb. 2003. Visual transduction by rod and cone photoreceptors. *In* Visual Neurosciences. L.M. Chalupa and J.S. Werner, editors. MIT Press, Cambridge, MA. 215–233.

Burnside, B., and N. Ackland. 1984. Effects of circadian rhythm and cAMP on retinomotor movements in the green sunfish, *Lepomis cyanellus*. *Invest. Ophthalmol. Vis. Sci.* 25:539–545.

Calderone, J.B., B.E. Reese, and G.H. Jacobs. 2003. Topography of photoreceptors and retinal ganglion cells in the spotted hyena (*Crocuta crocuta*). *Brain Behav. Evol.* 62:182–192. http://dx.doi.org/10.1159/000073270

Carter-Dawson, L.D., and M.M. LaVail. 1979. Rods and cones in the mouse retina. I. Structural analysis using light and electron microscopy. *J. Comp. Neurol.* 188:245–262. http://dx.doi.org/10.1002/cne.901880204

Cheng, C.L., and I. Novales Flamarique. 2007. Chromatic organization of cone photoreceptors in the retina of rainbow trout: single cones irreversibly switch from UV (SWS1) to blue (SWS2) light sensitive opsin during natural development. *J. Exp. Biol.* 210:4123–4135. http://dx.doi.org/10.1242/jeb.009217

Cheng, C.L., I. Novales Flamarique, F.I. Hárosi, J. Rickers-Haunerland, and N.H. Haunerland. 2006. Photoreceptor layer of salmonid fishes: transformation and loss of single cones in juvenile fish. *J. Comp. Neurol.* 495:213–235. http://dx.doi.org/10.1002/cne.20879

Cheng, C.L., K.J. Gan, and I. Novales Flamarique. 2007. The ultraviolet opsin is the first opsin expressed during retinal development of salmonid fishes. *Invest. Ophthalmol. Vis. Sci.* 48:866–873. http://dx.doi.org/10.1167/iovs.06-0442

Cheng, C.L., K.J. Gan, and I. Novales Flamarique. 2009. Thyroid hormone induces a time-dependent opsin switch in the retina of salmonid fishes. *Invest. Ophthalmol. Vis. Sci.* 50:3024–3032. http://dx.doi.org/10.1167/iovs.08-2713

Cohen, A.I. 1961. The fine structure of the extrafoveal receptors of the Rhesus monkey. *Exp. Eye Res.* 1:128–136. http://dx.doi.org/10.1016/S0014-4835(61)80018-3

Cohen, A.I. 1963. The fine structure of the visual receptors of the pigeon. *Exp. Eye Res.* 2:88–97. http://dx.doi.org/10.1016/S0014-4835(63)80028-7

Cohen, A.I. 1964. Some observations on the fine structure of the retinal receptors of the American gray squirrel. *Invest. Ophthalmol.* 3:198–216.

Collin, S.P. 2010. Evolution and ecology of retinal photoreception in early vertebrates. *Brain Behav. Evol.* 75:174–185. http://dx.doi.org/10.1159/000314904

Collin, S.P., and H.B. Collin. 1993. The visual system of the Florida garfish, *Lepisosteus platyrhincus* (Ginglymodi). I. Retina. *Brain Behav. Evol.* 42:77–97. http://dx.doi.org/10.1159/000114142

Collin, S.P., and H.B. Collin. 1998. Retinal and lenticular ultrastructure in the aestivating salamanderfish, *Lepidogalaxias salamandroides* (Galaxiidae, Teleostei) with special reference to a new type of photoreceptor mosaic. *Histol. Histopathol.* 13:1037–1048.

Collin, S.P., and H.B. Collin. 1999. The foveal photoreceptor mosaic in the pipefish, *Corythoichthyes paxtoni* (Syngnathidae, Teleostei). *Histol. Histopathol.* 14:369–382.

Collin, S.P., and I.C. Pottert. 2000. The ocular morphology of the southern hemisphere lamprey *Mordacia mordax* Richardson with special reference to a single class of photoreceptor and a retinal tapetum. *Brain Behav. Evol.* 55:120–138. http://dx.doi.org/10.1159/000006647

Collin, S.P., H.B. Collin, and M.A. Ali. 1996a. Ultrastructure and organisation of the retina and pigment epithelium in the cutlips minnow, *Exoglossum maxillingua* (Cyprinidae, Teleostei). *Histol. Histopathol.* 11:55–69.

Collin, S.P., H.B. Collin, and M.A. Ali. 1996b. Fine structure of the retina and pigment epithelium in the creek chub, *Semotilus atromaculatus* (Cyprinidae, Teleostei). *Histol. Histopathol.* 11:41–53.

Collin, S.P., R.V. Hoskins, and J.C. Partridge. 1998. Seven retinal specializations in the tubular eye of the deep-sea pearleye, *Scopelarchus michaelsarsi*: a case study in visual optimization. *Brain Behav. Evol.* 51:291–314. http://dx.doi.org/10.1159/000006544

Collin, S.P., I.C. Potter, and C.R. Braekevelt. 1999. The ocular morphology of the southern hemisphere lamprey *Geotria australis* gray, with special reference to optical specialisations and the characterisation and phylogeny of photoreceptor types. *Brain Behav. Evol.* 54:96–118. http://dx.doi.org/10.1159/000006616

Collin, S.P., N.S. Hart, J. Shand, and I.C. Potter. 2003. Morphology and spectral absorption characteristics of retinal photoreceptors in the southern hemisphere lamprey (*Geotria australis*). *Vis. Neurosci.* 20:119–130. http://dx.doi.org/10.1017/S0952523803202030

Collin, S.P., N.S. Hart, K.M. Wallace, J. Shand, and I.C. Potter. 2004. Vision in the southern hemisphere lamprey *Mordacia mordax*: spatial distribution, spectral absorption characteristics, and optical sensitivity of a single class of retinal photoreceptor. *Vis. Neurosci.* 21:765–773. http://dx.doi.org/10.1017/S0952523804215103

Crescitelli, F. 1972. The visual cells and visual pigments of the vertebrate eye. *In* Handbook of Sensory Physiology, Vol. VII/1, Photochemistry of Vision. H.J.A. Dartnall, editor. Springer-Verlag, New York. 245–363.

Cserháti, P., A. Szél, and P. Röhlich. 1989. Four cone types characterized by anti-visual pigment antibodies in the pigeon retina. *Invest. Ophthalmol. Vis. Sci.* 30:74–81.

Curcio, C.A., K.R. Sloan, R.E. Kalina, and A.E. Hendrickson. 1990. Human photoreceptor topography. *J. Comp. Neurol.* 292:497–523. http://dx.doi.org/10.1002/cne.902920402

Custer, N.V. 1973. Structurally specialized contacts between the photoreceptors of the retina of the axolotl. *J. Comp. Neurol.* 151: 35–56. http://dx.doi.org/10.1002/cne.901510104

Dartnall, H.J.A. 1972. Photosensitivity. *In* Handbook of Sensory Physiology, Vol. VII/1, Photochemistry of Vision. H.J.A. Dartnall, editor. Springer-Verlag, New York. 122–145.

Dartnall, H.J.A., C.F. Goodeve, and R.J. Lythgoe. 1936. The quantitative analysis of the photochemical bleaching of visual purple solutions in monochromatic light. *Proc. R. Soc. Lond. A.* 156:158–170. http://dx.doi.org/10.1098/rspa.1936.0141

Dearry, A., and R.B. Barlow Jr. 1987. Circadian rhythms in the green sunfish retina. *J. Gen. Physiol.* 89:745–770. http://dx.doi.org/10.1085/jgp.89.5.745

Dickson, D.H., and D.A. Graves. 1979. Fine structure of the lamprey photoreceptors and retinal pigment epithelium (*Petromyzon marinus* L.). *Exp. Eye Res.* 29:45–60. http://dx.doi.org/10.1016/0014-4835(79)90165-9

Dieterich, C.E., and J.W. Rohen. 1970. Über die Receptoren der Menschlichen Netzhaut. *Albrecht von Graefes Archiv fur Klinische und Experimentelle Ophthalmologie.* 179:235–258. http://dx.doi.org/10.1007/BF00410856

Douglas, R.H., and H.J. Wagner. 1982. Endogenous patterns of photomechanical movements in teleosts and their relation to activity rhythms. *Cell Tissue Res.* 226:133–144. http://dx.doi.org/10.1007/BF00217088

Dowling, J.E. 1965. Foveal receptors of the monkey retina: fine structure. *Science.* 147:57–59. http://dx.doi.org/10.1126/science.147.3653.57

Dubin, M.W., and L. Turner. 1977. Anatomy of the retina of the mink (*Mustela vison*). *J. Comp. Neurol.* 173:275–288. http://dx.doi.org/10.1002/cne.901730205

Dunn, R.F. 1966. Studies on the retina of the gecko *Coleonyx variegatus*. I. The visual cell classification. *J. Ultrastruct. Res.* 16:651–671. http://dx.doi.org/10.1016/S0022-5320(66)80012-6

Eckmiller, M.S. 1987. Cone outer segment morphogenesis: taper change and distal invaginations. *J. Cell Biol.* 105:2267–2277. http://dx.doi.org/10.1083/jcb.105.5.2267

Emond, M.P., R. McNeil, T. Cabana, C.G. Guerra, and P. Lachapelle. 2006. Comparing the retinal structures and functions in two species of gulls (*Larus delawarensis* and *Larus modestus*) with significant nocturnal behaviours. *Vision Res.* 46:2914–2925. http://dx.doi.org/10.1016/j.visres.2006.02.023

Engström, K. 1958. On the cone mosaic in the retina of *Parus major*. *Acta Zoologica (Stockholm, Sweden).* 39:65–69. http://dx.doi.org/10.1111/j.1463-6395.1958.tb00523.x

Engström, K. 1961. Cone types and cone arrangement in the retina of some gadids. *Acta Zoologica (Stockholm, Sweden).* 42:227–243. http://dx.doi.org/10.1111/j.1463-6395.1961.tb00064.x

Engström, K. 1963. Structure, organization and ultrastructure of the visual cells in the teleost family *Labridae*. *Acta Zoologica (Stockholm, Sweden).* 44:1–41. http://dx.doi.org/10.1111/j.1463-6395.1963.tb00399.x

Engström, K., and E. Rosstorp. 1963. Photomechanical responses in different cone types of *Leucisus rutilus*. *Acta Zoologica (Stockholm, Sweden).* 44:145–160. http://dx.doi.org/10.1111/j.1463-6395.1963.tb00406.x

Enoch, J.M. 1963. Optical properties of the retinal receptors. *Journal of the Optical Society of America.* 53:71–85. http://dx.doi.org/10.1364/JOSA.53.000071

Enoch, J.M., and H.E. Bedell. 1981. The Stiles-Crawford effects. *In* Vertebrate Photoreceptor Optics. J.M. Enoch and F.L. Tobey Jr., editors. Vol. 23. Springer-Verlag, New York. 83–126.

Evans, B.I., and R.D. Fernald. 1993. Retinal transformation at metamorphosis in the winter flounder (*Pseudopleuronectes americanus*). *Vis. Neurosci.* 10:1055–1064. http://dx.doi.org/10.1017/S0952523800010166

Fang, M., J. Li, W.H. Kwong, P. Kindler, G. Lu, S.M. Wai, and D.T. Yew. 2004. The complexity of the visual cells and visual pathways of the sturgeon. *Microsc. Res. Tech.* 65:122–129. http://dx.doi.org/10.1002/jemt.20112

Fein, A., and E.Z. Szuts. 1982. Photoreceptors: Their Role in Vision. Cambridge University Press, Cambridge, UK. 224 pp.

Fishelson, L., G. Ayalon, A. Zverdling, and R. Holzman. 2004. Comparative morphology of the eye (with particular attention to the retina) in various species of cardinal fish (Apogonidae, Teleostei). *Anat. Rec. A Discov. Mol. Cell. Evol. Biol.* 277:249–261.

Foelix, R.F., R. Kretz, and G. Rager. 1987. Structure and postnatal development of photoreceptors and their synapses in the retina of the tree shrew (*Tupaia belangeri*). *Cell Tissue Res.* 247:287–297. http://dx.doi.org/10.1007/BF00218310

Forsell, J., P. Ekström, I. Novales Flamarique, and B. Holmqvist. 2001. Expression of pineal ultraviolet- and green-like opsins in the pineal organ and retina of teleosts. *J. Exp. Biol.* 204:2517–2525.

Gall, M.D., and E. Fernández-Juricic. 2009. Effects of physical and visual access to prey on patch selection and food search effort in a sit-and-wait predator, the black phoebe. *The Condor.* 111:150–158. http://dx.doi.org/10.1525/cond.2009.080016

García, M., and J. de Juan. 1999. Fine structure of the retina of black bass, *Micropterus salmoides* (Centrarchidae, Teleostei). *Histol. Histopathol.* 14:1053–1065.

Gondo, M., and H. Ando. 1995. Comparative and histophysiological study of oil droplets in the avian retina. *Kobe J. Med. Sci.* 41:127–139.

Govardovskii, V.I., L.V. Zueva, and D.V. Lychakov. 1984. Microspectrophotometric study of visual pigments in five species of geckos. *Vision Res.* 24:1421–1423. http://dx.doi.org/10.1016/0042-6989(84)90198-6

Govardovskii, V.I., N.I. Chkheidze, and L.V. Zueva. 1988. Morphofunctional investigation of the retina in the crocodilian caiman *Caiman crocodilus*. *Sensory Systems.* 1:19–25.

Govardovskii, V.I., P. Röhlich, Á. Szél, and L.V. Zueva. 1992. Immunocytochemical reactivity of rod and cone visual pigments in the sturgeon retina. *Vis. Neurosci.* 8:531–537. http://dx.doi.org/10.1017/S0952523800005629

Gruber, S.H., and J.L. Cohen. 1985. Visual system of the white shark *Carcharodon carcharias*, with emphasis on retinal structure. *Memoirs of the Southern California Academy of Sciences.* 9:61–72.

Gruber, S.H., D.H. Hamasaki, and C.D.B. Bridges. 1963. Cones in the retina of the lemon shark (*Negaprion brevirostris*). *Vision Res.* 3:397–399. http://dx.doi.org/10.1016/0042-6989(63)90091-9

Gruber, S.H., R.L. Gulley, and J. Brandon. 1975. Duplex retina in seven elasmobranch species. *Bulletin of Marine Science.* 25:353–358.

Guma'a, S.A. 1982. Retinal development and retinomotor responses in perch, *Perca fluviatilis* L. *Journal of Fish Biology.* 20:611–618. http://dx.doi.org/10.1111/j.1095-8649.1982.tb03960.x

Hamasaki, D.I., and S.H. Gruber. 1965. The photoreceptors of the nurse shark, *Ginglymostoma cirratum* and the sting ray, *Dasyatis sayi*. *Bulletin of Marine Science.* 15:1051–1059.

Hannover, A. 1840. Über die Netzhaut und ihre Gehirnsubstanz bei Wirbelthieren, mit Ausnahme des Menschen. *Arch. Anat. Physiol. wissench. Med.* 1840:320–345.

Harahush, B.K., N.S. Hart, K. Green, and S.P. Collin. 2009. Retinal neurogenesis and ontogenetic changes in the visual system of the brown banded bamboo shark, *Chiloscyllium punctatum* (Hemiscyllidae, Elasmobranchii). *J. Comp. Neurol.* 513:83–97. http://dx.doi.org/10.1002/cne.21953

Hárosi, F.I. 1975. Absorption spectra and linear dichroism of some amphibian photoreceptors. *J. Gen. Physiol.* 66:357–382. http://dx.doi.org/10.1085/jgp.66.3.357

Hárosi, F.I. 1976. Spectral relations of cone pigments in goldfish. *J. Gen. Physiol.* 68:65–80. http://dx.doi.org/10.1085/jgp.68.1.65

Hárosi, F.I. 1982. Polarized microspectrophotometry for pigment orientation and concentration. *In* Methods in Enzymology, Vol. 81. Biomembranes, Part H, Visual Pigments and Purple Membranes. I. L. Packer, editor. Academic Press, New York. 642–647.

Hárosi, F.I. 1984. In vitro regeneration of visual pigment in isolated vertebrate photoreceptors. *In* Photoreceptors. A. Borsellino and L. Cervetto, editors. Plenum Press, New York. 41–63.

Hárosi, F.I. 1985. Ultraviolet- and violet-absorbing vertebrate visual pigments: dichroic and bleaching properties. *In* The Visual System: Proceedings of a Symposium in Honor of Edward F. MacNichol, Jr., Held in Woods Hole, Massachusetts, December 2 and 3, 1983. A. Fein and J.S. Levine, editors. Alan R. Liss, Inc., New York. 41–55.

Hárosi, F.I. 1987. Cynomolgus and rhesus monkey visual pigments. Application of Fourier transform smoothing and statistical techniques to the determination of spectral parameters. *J. Gen. Physiol.* 89:717–743. http://dx.doi.org/10.1085/jgp.89.5.717

Hárosi, F.I., and Y. Hashimoto. 1983. Ultraviolet visual pigment in a vertebrate: a tetrachromatic cone system in the dace. *Science.* 222:1021–1023. http://dx.doi.org/10.1126/science.6648514

Hárosi, F.I., and E.F. MacNichol Jr. 1974. Visual pigments of goldfish cones. Spectral properties and dichroism. *J. Gen. Physiol.* 63:279–304. http://dx.doi.org/10.1085/jgp.63.3.279

Hart, N.S., T.J. Lisney, N.J. Marshall, and S.P. Collin. 2004. Multiple cone visual pigments and the potential for trichromatic colour vision in two species of elasmobranch. *J. Exp. Biol.* 207:4587–4594. http://dx.doi.org/10.1242/jeb.01314

Hart, N.S., T.J. Lisney, and S.P. Collin. 2006. Cone photoreceptor oil droplet pigmentation is affected by ambient light intensity. *J. Exp. Biol.* 209:4776–4787. http://dx.doi.org/10.1242/jeb.02568

Haug, M.F., O. Biehlmaier, K.P. Mueller, and S.C.F. Neuhauss. 2010. Visual acuity in larval zebrafish: behavior and histology. *Front. Zool.* 7:8. http://dx.doi.org/10.1186/1742-9994-7-8

Hebel, R. 1971. Entwicklung und Struktur der Retina und des Tapetum lucidum des Hundes [Advances in Anatomy, Embryology and Cell Biology]. 45.2. Springer-Verlag. Berlin. 92 pp.

Hemmi, J.M., and U. Grünert. 1999. Distribution of photoreceptor types in the retina of a marsupial, the tammar wallaby (*Macropus eugenii*). *Vis. Neurosci.* 16:291–302. http://dx.doi.org/10.1017/S0952523899162102

Hendrickson, A., and D. Hicks. 2002. Distribution and density of medium- and short-wavelength selective cones in the domestic pig retina. *Exp. Eye Res.* 74:435–444. http://dx.doi.org/10.1006/exer.2002.1181

Hisatomi, O., and F. Tokunaga. 2002. Molecular evolution of proteins involved in vertebrate phototransduction. *Comp. Biochem. Physiol. B Biochem. Mol. Biol.* 133:509–522.

Hisatomi, O., S. Kayada, Y. Taniguchi, Y. Kobayashi, T. Satoh, and F. Tokunaga. 1998. Primary structure and characterization of a bullfrog visual pigment contained in small single cones. *Comp. Biochem. Physiol. B Biochem. Mol. Biol.* 119:585–591. http://dx.doi.org/10.1016/S0305-0491(98)00032-7

Hoang, Q.V., R.A. Linsenmeier, C.K. Chung, and C.A. Curcio. 2002. Photoreceptor inner segments in monkey and human retina: mitochondrial density, optics, and regional variation. *Vis. Neurosci.* 19:395–407. http://dx.doi.org/10.1017/S0952523802194028

Hodgkin, A.L., and P.M. O'Bryan. 1977. Internal recording of the early receptor potential in turtle cones. *J. Physiol.* 267:737–766.

Holcman, D., and J.I. Korenbrot. 2005. The limit of photoreceptor sensitivity: molecular mechanisms of dark noise in retinal cones. *J. Gen. Physiol.* 125:641–660. http://dx.doi.org/10.1085/jgp.200509277

Hollyfield, J.G., M.E. Rayborn, and J. Rosenthal. 1984. Two populations of rod photoreceptors in the retina of *Xenopus laevis* identified with 3H-fucose autoradiography. *Vision Res.* 24:777–782. http://dx.doi.org/10.1016/0042-6989(84)90148-2

Ishikawa, M., M. Takao, H. Washioka, F. Tokunaga, H. Watanabe, and A. Tonosaki. 1987. Demonstration of rod and cone photoreceptors in the lamprey retina by freeze-replication and immunofluorescence. *Cell Tissue Res.* 249:241–246. http://dx.doi.org/10.1007/BF00215506

Ishikawa, M., H. Watanabe, Y. Koike, O. Hisatomi, F. Tokunaga, and A. Tonosaki. 1989. Demonstration by lectin cytochemistry of rod and cone photoreceptors in the lamprey retina. *Cell Tissue Res.* 256:227–232. http://dx.doi.org/10.1007/BF00218879

Ives, J.T., R.A. Normann, and P.W. Barber. 1983. Light intensification by cone oil droplets: electromagnetic considerations. *Journal of the Optical Society of America.* 73:1725–1731. http://dx.doi.org/10.1364/JOSA.73.001725

Januschka, M.M., D.A. Burkhardt, S.L. Erlandsen, and R.L. Purple. 1987. The ultrastructure of cones in the walleye retina. *Vision Res.* 27:327–341. http://dx.doi.org/10.1016/0042-6989(87)90082-4

Johnson, B.K., and K. Tansley. 1956. The cones of the grass snake's eye. *Nature.* 178:1285–1286. http://dx.doi.org/10.1038/1781285a0

Jones, A.E. 1965. The retinal structure of (*Aotes trivirgatus*) the owl monkey. *J. Comp. Neurol.* 125:19–27. http://dx.doi.org/10.1002/cne.901250104

Kalberer, M., and C. Pedler. 1963. The visual cells of the alligator: an electron microscopic study. *Vision Res.* 61:323–329. http://dx.doi.org/10.1016/0042-6989(63)90006-3

Keefe, J.R. 1971. The fine structure of the retina in the newt, *Triturus viridescens*. *J. Exp. Zool.* 177:263–293. http://dx.doi.org/10.1002/jez.1401770302

Kenkre, J.S., N.A. Moran, T.D. Lamb, and O.A. Mahroo. 2005. Extremely rapid recovery of human cone circulating current at the extinction of bleaching exposures. *J. Physiol.* 567:95–112. http://dx.doi.org/10.1113/jphysiol.2005.088468

Kim, J., E. Lee, B.S. Chang, C.S. Oh, G.H. Mun, Y.H. Chung, and D.H. Shin. 2005. The presence of megamitochondria in the ellipsoid of photoreceptor inner segment of the zebrafish retina. *Anat. Histol. Embryol.* 34:339–342. http://dx.doi.org/10.1111/j.1439-0264.2005.00612.x

Kim, T.J., Y.K. Jeon, J.Y. Lee, E.S. Lee, and C.J. Jeon. 2008. The photoreceptor populations in the retina of the greater horseshoe bat *Rhinolophus ferrumequinum*. *Mol. Cells.* 26:373–379.

Kinney, M.S., and S.K. Fisher. 1978a. The photoreceptors and pigment epithelium of the adult *Xenopus* retina: morphology and outer segment renewal. *Proc. R. Soc. Lond. B.* 201:131–147. http://dx.doi.org/10.1098/rspb.1978.0036

Kinney, M.S., and S.K. Fisher. 1978b. The photoreceptors and pigment epithelium of the larval *Xenopus* retina: morphogenesis and outer segment renewal. *Proc. R. Soc. Lond. B Biol. Sci.* 201:149–167. http://dx.doi.org/10.1098/rspb.1978.0037

Knabe, W., S. Skatchkov, and H.J. Kuhn. 1997. "Lens mitochondria" in the retinal cones of the tree-shrew *Tupaia belangeri*. *Vision Res.* 37:267–271. http://dx.doi.org/10.1016/S0042-6989(96)00199-X

Kohbara, J., H. Niwa, and M. Oguri. 1987. Comparative light microscopic studies on the retina of some elasmobranch fishes. *Nippon Suisan Gakkaishi.* 53:2117–2125. http://dx.doi.org/10.2331/suisan.53.2117

Kojima, D., T. Okano, Y. Fukada, Y. Shichida, T. Yoshizawa, and T.G. Ebrey. 1992. Cone visual pigments are present in gecko rod cells. *Proc. Natl. Acad. Sci. USA.* 89:6841–6845. http://dx.doi.org/10.1073/pnas.89.15.6841

Kolb, H., and J. Jones. 1982. Light and electron microscopy of the photoreceptors in the retina of the red-eared slider, *Pseudemys scripta elegans*. *J. Comp. Neurol.* 209:331–338. http://dx.doi.org/10.1002/cne.902090402

Kolb, H., and J. Jones. 1987. The distinction by light and electron microscopy of two types of cone containing colorless oil droplets in the retina of the turtle. *Vision Res.* 27:1445–1458. http://dx.doi.org/10.1016/0042-6989(87)90154-4

Konishi, T. 1965. Developmental studies on the retinal oil globules in Japanese quail, *Coturnix coturnix Japonica*. *Dobutsugaku Zasshi.* 74:119–131.

Kühne, J.H. 1983. Rod receptors in the retina of *Tupaia belangeri*. *Anat. Embryol. (Berl.).* 167:95–102. http://dx.doi.org/10.1007/BF00304603

Kunz, Y.W., S. Ennis, and C. Wise. 1983. Ontogeny of the photoreceptors in the embryonic retina of the viviparous guppy, *Poecilia reticulata* P. (Teleostei). An electron-microscopical study. *Cell Tissue Res.* 230:469–486. http://dx.doi.org/10.1007/BF00216193

Kunz, Y.W., M. Ni Shuilleabhain, and E. Callaghan. 1985. The eye of the venomous marine teleost *Trachinus vipera* with special reference to the structure and ultrastructure of visual cells and pigment epithelium. *Exp. Biol.* 43:161–178.

Kusmic, C., and P. Gualtieri. 2000. Morphology and spectral sensitivities of retinal and extraretinal photoreceptors in freshwater teleosts. *Micron.* 31:183–200. http://dx.doi.org/10.1016/S0968-4328(99)00081-5

Land, M.F. 1979. The optical mechanism of the eye of *Limulus*. *Nature.* 280:396–397. http://dx.doi.org/10.1038/280396a0

Leach, E.H. 1963. On the structure of the retina of man and monkey. *J. R. Microsc. Soc.* 82:135–143. http://dx.doi.org/10.1111/j.1365-2818.1963.tb05311.x

Leeper, H.F. 1978. Horizontal cells of the turtle retina. II. Analysis of interconnections between photoreceptor cells and horizontal cells by light microscopy. *J. Comp. Neurol.* 182:795–809. http://dx.doi.org/10.1002/cne.901820504

Levi-Setti, R., D.A. Park, and R. Winston. 1975. The corneal cones of *Limulus* as optimised light concentrators. *Nature.* 253:115–116. http://dx.doi.org/10.1038/253115a0

Liebman, P.A., and A.M. Granda. 1971. Microspectrophotometric measurements of visual pigments in two species of turtle, *Pseudemys scripta* and *Chelonia mydas*. *Vision Res.* 11:105–114. http://dx.doi.org/10.1016/0042-6989(71)90227-6

Litherland, L., and S.P. Collin. 2008. Comparative visual function in elasmobranchs: spatial arrangement and ecological correlates of photoreceptor and ganglion cell distributions. *Vis. Neurosci.* 25:549–561. http://dx.doi.org/10.1017/S0952523808080693

Locket, N.A. 1973. Retinal structure in *Latimeria chalumnae*. *Philos. Trans. R. Soc. Lond. B Biol. Sci.* 266:493–518. http://dx.doi.org/10.1098/rstb.1973.0054

Locket, A. 1977. Adaptations to the deep-sea environment. *In* Handbook of Sensory Physiology, Vol. VIII/5, The Visual System in Vertebrates. F. Crescitelli, editor. Springer-Verlag, Berlin. 67–193.

Loew, E.R., V.I. Govardovskii, P. Röhlich, and Á. Szél. 1996. Microspectrophotometric and immunocytochemical identification of ultraviolet photoreceptors in geckos. *Vis. Neurosci.* 13:247–256. http://dx.doi.org/10.1017/S0952523800007483

Ma, J.X., S. Znoiko, K.L. Othersen, J.C. Ryan, J. Das, T. Isayama, M. Kono, D.D. Oprian, D.W. Corson, M.C. Cornwall, et al. 2001. A visual pigment expressed in both rod and cone photoreceptors. *Neuron.* 32:451–461. http://dx.doi.org/10.1016/S0896-6273(01)00482-2

MacNichol, E.F., Jr., Y.W. Kunz, J.S. Levine, F.I. Hárosi, and B.A. Collins. 1978. Ellipsosomes: organelles containing a cytochrome-like pigment in the retinal cones of certain fishes. *Science.* 200:549–552. http://dx.doi.org/10.1126/science.644317

Mariani, A.P. 1986. Photoreceptors of the larval tiger salamander retina. *Proc. R. Soc. Lond. B Biol. Sci.* 227:483–492. http://dx.doi.org/10.1098/rspb.1986.0035

Mariani, A.P., and A.E. Leure-duPree. 1978. Photoreceptors and oil droplet colors in the red area of the pigeon retina. *J. Comp. Neurol.* 182:821–837. http://dx.doi.org/10.1002/cne.901820506

Martin, G., L.M. Rojas, Y. Ramírez, and R. McNeil. 2004. The eyes of oilbirds (*Steatornis caripensis*): pushing at the limits of sensitivity. *Naturwissenschaften.* 91:26–29. http://dx.doi.org/10.1007/s00114-003-0495-3

McFarland, W.N., and E.R. Loew. 1983. Wave produced changes in underwater light and their relation to vision. *Environmental Biology of Fishes.* 8:173–184. http://dx.doi.org/10.1007/BF00001083

McNeil, R., A. McSween, and P. Lachapelle. 2005. Comparison of the retinal structure and function in four bird species as a function of the time they start singing in the morning. *Brain Behav. Evol.* 65:202–214. http://dx.doi.org/10.1159/000083881

Meyer, D.B., and H.C. May Jr. 1973. The topographical distribution of rods and cones in the adult chicken retina. *Exp. Eye Res.* 17:347–355. http://dx.doi.org/10.1016/0014-4835(73)90244-3

Meyer-Rochow, V.B., and M.A. Klyne. 1982. Retinal organization of the eyes of three nototheniid fishes from the Ross Sea (Antarctica). *Gegenbaurs Morphol. Jahrb.* 128:762–777.

Meyer-Rochow, V.B., S. Wohlfahrt, and P.K. Ahnelt. 2005. Photoreceptor cell types in the retina of the tuatara (*Sphenodon punctatus*) have cone characteristics. *Micron.* 36:423–428. http://dx.doi.org/10.1016/j.micron.2005.03.009

Missotten, L. 1966. The Ultrastructure of the Human Retina. Éditions Arscia & Presses Académiques Européennes, Bruxelles. 184 pp.

Moody, M.F., and J.D. Robertson. 1960. The fine structure of some retinal photoreceptors. *J. Biophys. Biochem. Cytol.* 7:87–92. http://dx.doi.org/10.1083/jcb.7.1.87

Moore, G.A., H.R. Pollock, and D. Lima. 1950. The visual cells of *Ericymba buccata* (Cope). *J. Comp. Neurol.* 93:289–295. http://dx.doi.org/10.1002/cne.900930209

Müller, H. 1856. Anatomisch-physiologishe Untersuchungen über die Retina bei Menschen und Wirbelthieren. *Zeits. f. wiss. Zool.* 8:1–122.

Müller, H. 1952. Bau und Wachstum der Netzhaut des Guppy (*Lebistes reticulates*). *Zool. Jb. Abt. Allg. Zool. Physiol.* 63:275–324.

Müller, B., and L. Peichl. 1989. Topography of cones and rods in the tree shrew retina. *J. Comp. Neurol.* 282:581–594. http://dx.doi.org/10.1002/cne.902820409

Müller, B., S.M. Goodman, and L. Peichl. 2007. Cone photoreceptor diversity in the retinas of fruit bats (*megachiroptera*). *Brain Behav. Evol.* 70:90–104. http://dx.doi.org/10.1159/000102971

Müller, B., M. Glösmann, L. Peichl, G.C. Knop, C. Hagemann, and J. Ammermüller. 2009. Bat eyes have ultraviolet-sensitive cone photoreceptors. *PLoS ONE.* 4:e6390. http://dx.doi.org/10.1371/journal.pone.0006390

Munk, O. 1977. The visual cells and retinal tapetum of the foveate deep-sea fish *Scopelosaurus lepidus* (Teleostei). *Zoomorphology.* 87:21–49. http://dx.doi.org/10.1007/BF02568740

Munk, O. 1985. Retinal cones of the snake mackerel, *Gempylus serpens.* Cuvier, 1829. *Videnskr. Meddr. Dansk Naturh. Foren.* 146:7–20.

Munz, F.W., and W.N. McFarland. 1977. Evolutionary adaptations of fishes to the photic environment. *In* Handbook of Sensory Physiology, Vol II/5, The Visual System of Vertebrates. F. Crescitelli, editor. Springer-Verlag, Berlin. 193–274.

Muradov, H., V. Kerov, K.K. Boyd, and N.O. Artemyev. 2008. Unique transducins expressed in long and short photoreceptors of lamprey *Petromyzon marinus*. *Vision Res.* 48:2302–2308. http://dx.doi.org/10.1016/j.visres.2008.07.006

Murray, R.G., A.E. Jones, and A. Murray. 1973. Fine structure of photoreceptors in the owl monkey. *Anat. Rec.* 175:673–695. http://dx.doi.org/10.1002/ar.1091750404

Nawrocki, L., R. BreMiller, G. Streisinger, and M. Kaplan. 1985. Larval and adult visual pigments of the zebrafish, *Brachydanio rerio*. *Vision Res.* 25:1569–1576. http://dx.doi.org/10.1016/0042-6989(85)90127-0

Neave, D.A. 1984. The development of the retinomotor reactions in larval plaice (*Pleuronectes platessa*, L.) and turbot (*Scophthalmus maximus*, L.). *Journal of Experimental Marine Biology and Ecology.* 76:167–175. http://dx.doi.org/10.1016/0022-0981(84)90064-9

Nilsson, S.E.G. 1964. An electron microscopic classification of the retinal receptors of the leopard frog (*Rana pipiens*). *J. Ultrastruct. Res.* 10:390–416. http://dx.doi.org/10.1016/S0022-5320(64)80018-6

Nilsson, S.E.G. 1965. The ultrastructure of the receptor outer segments in the retina of the leopard frog (*Rana pipiens*). *J. Ultrastruct. Res.* 12:207–231. http://dx.doi.org/10.1016/S0022-5320(65)80016-8

Nordby, K., and L.T. Sharpe. 1988. The directional sensitivity of the photoreceptors in the human achromat. *J. Physiol.* 399:267–281.

Novales Flamarique, I. 2002. Partial re-incorporation of corner cones in the retina of the Atlantic salmon (*Salmo salar*). *Vision Res.* 42:2737–2745. http://dx.doi.org/10.1016/S0042-6989(02)00360-7

Novales Flamarique, I. 2005. Temporal shifts in visual pigment absorbance in the retina of Pacific salmon. *J. Comp. Physiol. A Neuroethol. Sens. Neural Behav. Physiol.* 191:37–49. http://dx.doi.org/10.1007/s00359-004-0573-9

Novales Flamarique, I. 2011. Unique photoreceptor arrangements in a fish with polarized light discrimination. *J. Comp. Neurol.* 519:714–737. http://dx.doi.org/10.1002/cne.22544

Novales Flamarique, I., and F.I. Hárosi. 1997. Photoreceptor morphology and visual pigment content in the retina of the common white sucker (*Catostomus commersoni*). *The Biological Bulletin.* 193:209–210.

Novales Flamarique, I., and F.I. Hárosi. 2000. Photoreceptors, visual pigments, and ellipsosomes in the killifish, *Fundulus heteroclitus*: a microspectrophotometric and histological study. *Vis. Neurosci.* 17:403–420. http://dx.doi.org/10.1017/S0952523800173080

Novales Flamarique, I., and C.W. Hawryshyn. 1998. The common white sucker (*Catostomus commersoni*): a fish with ultraviolet sensitivity that lacks polarization sensitivity. *J. Comp. Physiol. A.* 182: 331–341. http://dx.doi.org/10.1007/s003590050183

Novales Flamarique, I., G.A. Mueller, C.L. Cheng, and C.R. Figiel. 2007. Communication using eye roll reflective signalling. *Proc. Biol. Sci.* 274:877–882. http://dx.doi.org/10.1098/rspb.2006.0246

O'Brien, B. 1946. A theory of the Stiles and Crawford effect. *J. Opt. Soc. Am.* 36:506–509. http://dx.doi.org/10.1364/JOSA.36.000506

O'Brien, B. 1951. Vision and resolution in the central retina. *J. Opt. Soc. Am.* 41:882–894. http://dx.doi.org/10.1364/JOSA.41.000882

Ogden, T.E. 1975. The receptor mosaic of *Aotes trivirgatus*: distribution of rods and cones. *J. Comp. Neurol.* 163:193–202. http://dx.doi.org/10.1002/cne.901630205

Ohtsuka, T. 1985. Spectral sensitivities of seven morphological types of photoreceptors in the retina of the turtle, *Geoclemys reevesii*. *J. Comp. Neurol.* 237:145–154. http://dx.doi.org/10.1002/cne.902370202

Ohtsuka, T., and K. Kawamata. 1990. Monoclonal antibody labels both rod and cone outer segments of turtle photoreceptors. *Exp. Eye Res.* 50:483–486. http://dx.doi.org/10.1016/0014-4835(90)90036-T

Oishi, T., A. Kawata, T. Hayashi, Y. Fukada, Y. Shichida, and T. Yoshizawa. 1990. Immunohistochemical localization of iodopsin in the retina of the chicken and Japanese quail. *Cell and Tissue Research.* 261:397–401. http://dx.doi.org/10.1007/BF00313517

Packer, O., A.E. Hendrickson, and C.A. Curcio. 1989. Photoreceptor topography of the retina in the adult pigtail macaque (*Macaca nemestrina*). *J. Comp. Neurol.* 288:165–183. http://dx.doi.org/10.1002/cne.902880113

Paillart, C., K. Zhang, T.I. Rebrik, W. Baehr, and J.I. Korenbrot. 2006. Cloning and molecular characterization of cGMP-gated ion channels from rod and cone photoreceptors of striped bass (*M. saxatilis*) retina. *Vis. Neurosci.* 23:99–113. http://dx.doi.org/10.1017/S0952523806231092

Palacios, A.G., F. Bozinovic, A. Vielma, C.A. Arrese, D.M. Hunt, and L. Peichl. 2010. Retinal photoreceptor arrangement, SWS1 and LWS opsin sequence, and electroretinography in the South American marsupial *Thylamys elegans* (Waterhouse, 1839). *J. Comp. Neurol.* 518:1589–1602. http://dx.doi.org/10.1002/cne.22292

Pedler, C. 1965. Duplicity theory and microstructure of the retina: rods and cones - a fresh approach. *In* Colour Vision: Physiology and Experimental Psychology; Ciba Foundation Symposium. A.V.S. de Reuck and J. Knight, editors. Little, Brown & Co., Boston. 52–88.

Pedler, C., and K. Tansley. 1963. The fine structure of the cone of a diurnal gecko (*Phelsuma inuguis*). *Exp. Eye Res.* 2:39–47. http://dx.doi.org/10.1016/S0014-4835(63)80023-8

Pedler, C., and R. Tilly. 1964. The nature of the Gecko visual cell. A light and electron microscopic study. *Vision Res.* 4:499–510. http://dx.doi.org/10.1016/0042-6989(64)90056-2

Peichl, L. 2005. Diversity of mammalian photoreceptor properties: adaptations to habitat and lifestyle? *Anat. Rec. A Discov. Mol. Cell. Evol. Biol.* 287:1001–1012.

Peichl, L.G.B., G. Behrmann, and R.H. Kröger. 2001. For whales and seals the ocean is not blue: a visual pigment loss in marine mammals. *Eur. J. Neurosci.* 13:1520–1528. http://dx.doi.org/10.1046/j.0953-816x.2001.01533.x

Petry, H.M., and F.I. Hárosi. 1990. Visual pigments of the tree shrew (*Tupaia belangeri*) and greater galago (*Galago crassicaudatus*): a microspectrophotometric investigation. *Vision Res.* 30:839–851. http://dx.doi.org/10.1016/0042-6989(90)90053-N

Petry, H.M., J.T. Erichsen, and Á. Szél. 1993. Immunocytochemical identification of photoreceptor populations in the tree shrew retina. *Brain Res.* 616:344–350. http://dx.doi.org/10.1016/0006-8993(93)90230-K

Pietzsch-Rohrschneider, I. 1976. Scanning electron microscopy of photoreceptor cells in the light- and dark-adapted retina of *Haplochromis burtoni* (Cichlidae, Teleostei). *Cell Tissue Res.* 175:123–130. http://dx.doi.org/10.1007/BF00220828

Reckel, F., and R.R. Melzer. 2003. Regional variations in the outer retina of atherinomorpha (Beloniformes, Atheriniformes, Cyprinodontiformes: Teleostei): photoreceptors, cone patterns, and cone densities. *J. Morphol.* 257:270–288. http://dx.doi.org/10.1002/jmor.10122

Reckel, F., R.R. Melzer, and U. Smola. 1999. Ultrastructure of the retina of two subspecies of *Coregonus lavaretus* (Teleostei) from Lake Constance (Germany). *Acta Zoologica (Stockholm, Sweden).* 80:153–162. http://dx.doi.org/10.1046/j.1463-6395.1999.80220013.x

Reckel, F., R.R. Melzer, and U. Smola. 2001. Outer retinal fine structure of the garfish *Belone belone* (L.) (Belonidae, Teleostei) during light and dark adaptation – photoreceptors, cone patterns and densities. *Acta Zoologica (Stockholm, Sweden).* 82:89–105. http://dx.doi.org/10.1046/j.1463-6395.2001.00071.x

Reckel, F., R.R. Melzer, J.W. Parry, and J.K. Bowmaker. 2002. The retina of five atherinomorph teleosts: photoreceptors, patterns and spectral sensitivities. *Brain Behav. Evol.* 60:249–264. http://dx.doi.org/10.1159/000067191

Reckel, F., B. Hoffmann, R.R. Melzer, J. Horppila, and U. Smola. 2003. Photoreceptors and cone patterns in the retina of the smelt *Osmerus eperlanus* (L.) (Osmeridae: Teleostei). *Acta Zoologica (Stockholm, Sweden).* 84:161–170. http://dx.doi.org/10.1046/j.1463-6395.2003.00142.x

Reichenbach, A., and U. Fuchs. 1983. Photoreceptor layer composition in the retina of the frog (*Rana esculenta*). *Gegenbaurs Morphol. Jahrb.* 129:299–305.

Rieke, F., and D.A. Baylor. 1996. Molecular origin of continuous dark noise in rod photoreceptors. *Biophys. J.* 71:2553–2572. http://dx.doi.org/10.1016/S0006-3495(96)79448-1

Rieke, F., and D.A. Baylor. 2000. Origin and functional impact of dark noise in retinal cones. *Neuron.* 26:181–186. http://dx.doi.org/10.1016/S0896-6273(00)81148-4

Rocha, F.A., P.K. Ahnelt, L. Peichl, C.A. Saito, L.C.L. Silveira, and S.M.A. De Lima. 2009. The topography of cone photoreceptors in the retina of a diurnal rodent, the agouti (*Dasyprocta aguti*). *Vis. Neurosci.* 26:167–175. http://dx.doi.org/10.1017/S095252380808098X

Röhlich, P., and Á. Szél. 2000. Photoreceptor cells in the *Xenopus* retina. *Microsc. Res. Tech.* 50:327–337. http://dx.doi.org/10.1002/1097-0029(20000901)50:5<327::AID-JEMT2>3.0.CO;2-P

Röhlich, P., Á. Szél, and D.S. Papermaster. 1989. Immunocytochemical reactivity of *Xenopus laevis* retinal rods and cones with several monoclonal antibodies to visual pigments. *J. Comp. Neurol.* 290:105–117. http://dx.doi.org/10.1002/cne.902900107

Rojas, L.M., R. McNeil, T. Cabana, and P. Lachapelle. 1999a. Behavioral, morphological and physiological correlates of diurnal and nocturnal vision in selected wading bird species. *Brain Behav. Evol.* 53:227–242. http://dx.doi.org/10.1159/000006596

Rojas, L.M., R. McNeil, T. Cabana, and P. Lachapelle. 1999b. Diurnal and nocturnal visual capabilities in shorebirds as a function of their feeding strategies. *Brain Behav. Evol.* 53:29–43. http://dx.doi.org/10.1159/000006580

Rojas, L.M., Y. Ramírez, R. McNeil, M. Mitchell, and G. Marín. 2004. Retinal morphology and electrophysiology of two caprimulgiformes birds: the cave-living and nocturnal oilbird (*Steatornis caripensis*), and the crepuscularly and nocturnally foraging common pauraque (*Nyctidromus albicollis*). *Brain Behav. Evol.* 64:19–33. http://dx.doi.org/10.1159/000077540

Rojas, L.M., M.A. Mitchell, Y.M. Ramírez, and R. McNeil. 2007. Comparative analysis of retina structure and photopic electroretinograms in developing altricial pigeons (*Columba livia*) and precocial Japanese quails (*Coturnix coturnix Japonica*). *Neotrop. Ornitholog. Soc.* 18:503–518.

Röll, B. 2001. Retina of Bouton's skink (Reptilia, Scincidae): visual cells, fovea, and ecological constraints. *J. Comp. Neurol.* 436:487–496. http://dx.doi.org/10.1002/cne.1082

Rushton, W.A.H. 1965. The Ferrier Lecture, 1962. Visual adaptation. *Proc. R. Soc. Lond. B.* 162:20–46. http://dx.doi.org/10.1098/rspb.1965.0024

Sampath, A.P., and D.A. Baylor. 2002. Molecular mechanism of spontaneous pigment activation in retinal cones. *Biophys. J.* 83:184–193. http://dx.doi.org/10.1016/S0006-3495(02)75160-6

Schnapf, J.L. 1983. Dependence of the single photon response on longitudinal position of absorption in toad rod outer segments. *J. Physiol.* 343:147–159.

Schultze, M. 1866. Zur Anatomie und Physiologie der Retina. *Archiv für Mikroskopische Anatomie.* 2:175–286. http://dx.doi.org/10.1007/BF02962033

Schultze, M. 1867. Über Stäbchen und Zapfen der Retina. *Archiv für Mikroskopische Anatomie.* 3:215–247. http://dx.doi.org/10.1007/BF02960456

Shand, J., M.A. Archer, and S.P. Collin. 1999. Ontogenetic changes in the retinal photoreceptor mosaic in a fish, the black bream, *Acanthopagrus butcheri*. *J. Comp. Neurol.* 412:203–217. http://dx.doi.org/10.1002/(SICI)1096-9861(19990920)412:2<203::AID-CNE2>3.0.CO;2-3

Shand, J., M.A. Archer, N. Thomas, and J. Cleary. 2001. Retinal development of West Australian dhufish, *Glaucosoma hebraicum*. *Vis. Neurosci.* 18:711–724. http://dx.doi.org/10.1017/S0952523801185056

Sherry, D.M., D.D. Bui, and W.J. Degrip. 1998. Identification and distribution of photoreceptor subtypes in the neotenic tiger salamander retina. *Vis. Neurosci.* 15:1175–1187. http://dx.doi.org/10.1017/S0952523898156201

Shively, J.N., G.P. Epling, and R. Jensen. 1970. Fine structure of the canine eye: retina. *Am. J. Vet. Res.* 31:1339–1359.

Sillman, A.J., and D.A. Dahlin. 2004. Photoreceptor topography in the duplex retina of the paddlefish (*Polydon spathula*). *Journal of Experimental Zoology Part A: Comparative Experimental Biology.* 301A:674–681. http://dx.doi.org/10.1002/jez.a.63

Sillman, A.J., S.J. Ronan, and E.R. Loew. 1991. Histology and microspectrophotometry of the photoreceptors of a crocodilian, *Alligator mississippiensis*. *Proc. R. Soc. Lond. B.* 243:93–98. http://dx.doi.org/10.1098/rspb.1991.0016

Sillman, A.J., S.J. Ronan, and E.R. Loew. 1993. Scanning electron microscopy and microspectrophotometry of the photoreceptors of ictalurid catfishes. *J. Comp. Physiol. A Neuroethol. Sens. Neural Behav. Physiol.* 173:801–807. http://dx.doi.org/10.1007/BF02451910

Sillman, A.J., V.I. Govardovskii, P. Röhlich, J.A. Southard, and E.R. Loew. 1997. The photoreceptors and visual pigments of the garter snake (*Thamnophis sirtalis*): a microspectrophotometric, scanning electron microscopic and immunocytochemical study. *J. Comp. Physiol. A Neuroethol. Sens. Neural Behav. Physiol.* 181:89–101. http://dx.doi.org/10.1007/s003590050096

Sillman, A.J., C.J. O'Leary, C.D. Tarantino, and E.R. Loew. 1999a. The photoreceptors and visual pigments of two species of Acipenseriformes, the shovelnose sturgeon (*Scaphirhynchus platorynchus*) and the paddlefish *(Polyodon spathula*). *J. Comp. Physiol. A Neuroethol. Sens. Neural Behav. Physiol.* 184:37–47. http://dx.doi.org/10.1007/s003590050304

Sillman, A.J., J.K. Carver, and E.R. Loew. 1999b. The photoreceptors and visual pigments in the retina of a boid snake, the ball python (*Python regius*). *J. Exp. Biol.* 202:1931–1938.

Sillman, A.J., J.L. Johnson, and E.R. Loew. 2001. Retinal photoreceptors and visual pigments in *Boa constrictor imperator*. *J. Exp. Zool.* 290:359–365. http://dx.doi.org/10.1002/jez.1076

Sillman, A.J., A.K. Beach, D.A. Dahlin, and E.R. Loew. 2005. Photoreceptors and visual pigments in the retina of the fully anadromous green sturgeon (*Acipenser medirostrus*) and the potamodromous pallid sturgeon (*Scaphirhynchus albus*). *J. Comp. Physiol. A Neuroethol. Sens. Neural Behav. Physiol.* 191:799–811. http://dx.doi.org/10.1007/s00359-005-0004-6

Singarajah, K.V., and F.I. Hárosi. 1992. Visual cells and pigments in a demersal fish, the black sea bass (*Centropristis striata*). *The Biological Bulletin.* 182:135–144. http://dx.doi.org/10.2307/1542188

Snyder, A.W., and R. Menzel. 1975. Photoreceptor Optics. Springer-Verlag, New York. 523 pp.

Snyder, A.W., and W.H. Miller. 1977. Photoreceptor diameter and spacing for highest resolving power. *J. Opt. Soc. Am.* 67:696–698. http://dx.doi.org/10.1364/JOSA.67.000696

Snyder, A.W., and C. Pask. 1973. The Stiles-Crawford effect—explanation and consequences. *Vision Res.* 13:1115–1137. http://dx.doi.org/10.1016/0042-6989(73)90148-X

Solovei, I., M. Kreysing, C. Lanctôt, S. Kösem, L. Peichl, T. Cremer, J. Guck, and B. Joffe. 2009. Nuclear architecture of rod photoreceptor cells adapts to vision in mammalian evolution. *Cell.* 137:356–368. http://dx.doi.org/10.1016/j.cell.2009.01.052

Steinberg, R.H., M. Reid, and P.L. Lacy. 1973. The distribution of rods and cones in the retina of the cat (*Felis domesticus*). *J. Comp. Neurol.* 148:229–248. http://dx.doi.org/10.1002/cne.901480209

Steinberg, R.H., I. Wood, and M.J. Hogan. 1977. Pigment epithelial ensheathment and phagocytosis of extrafoveal cones in human retina. *Philos. Trans. R. Soc. Lond. B Biol. Sci.* 277:459–474. http://dx.doi.org/10.1098/rstb.1977.0028

Stell, W.K. 1972. The structure and morphologic relations of rods and cones in the retina of the spiny dogfish, *Squalus. Comp. Biochem. Physiol. A.* 42:141–151. http://dx.doi.org/10.1016/0300-9629(72)90374-X

Stell, W.K., and F.I. Hárosi. 1976. Cone structure and visual pigment content in the retina of the goldfish. *Vision Res.* 16:647–657. http://dx.doi.org/10.1016/0042-6989(76)90013-4

Stiles, W.S., and B.H. Crawford. 1933. The luminous efficiency of rays entering the eye pupil at different points. *Proc. R. Soc. Lond. B.* 112:428–450. http://dx.doi.org/10.1098/rspb.1933.0020

Szél, Á., L. Takács, É. Monostori, T. Diamantstein, I. Vigh-Teichmann, and P. Röhlich. 1986. Monoclonal antibody-recognizing cone visual pigment. *Exp. Eye Res.* 43:871–883. http://dx.doi.org/10.1016/0014-4835(86)90066-7

Szél, Á., T. Diamantstein, and P. Röhlich. 1988. Identification of the blue-sensitive cones in the mammalian retina by anti-visual pigment antibody. *J. Comp. Neurol.* 273:593–602. http://dx.doi.org/10.1002/cne.902730413

Theiss, S.M., T.J. Lisney, S.P. Collin, and N.S. Hart. 2007. Colour vision and visual ecology of the blue-spotted maskray, *Dasyatis kuhlii* Müller & Henle, 1814. *J. Comp. Physiol. A Neuroethol. Sens. Neural Behav. Physiol.* 193:67–79. http://dx.doi.org/10.1007/s00359-006-0171-0

Thomas, M.M., and T.D. Lamb. 1999. Light adaptation and dark adaptation of human rod photoreceptors measured from the *a*-wave of the electroretinogram. *J. Physiol.* 518:479–496. http://dx.doi.org/10.1111/j.1469-7793.1999.0479p.x

van der Meer, H.J. 1992. Constructional morphology of photoreceptor patterns in percomorph fish. *Acta Biotheoretica.* 40:51–85. http://dx.doi.org/10.1007/BF00046551

Vorobyev, M. 2003. Coloured oil droplets enhance colour discrimination. *Proc. Biol. Sci.* 270:1255–1261. http://dx.doi.org/10.1098/rspb.2003.2381

Wagner, H.J. 1978. Cell types and connectivity patterns in mosaic retinas. Springer-Verlag, Berlin. 81 pp.

Walls, G.L. 1963. The Vertebrate Eye and its Adaptive Radiation. Hafner Publishing Co., New York. 785 pp.

Wang, Q., X. Zhang, L. Zhang, F. He, G. Zhang, M. Jamrich, and T.G. Wensel. 2008. Activation-dependent hindrance of photoreceptor G protein diffusion by lipid microdomains. *J. Biol. Chem.* 283:30015–30024. http://dx.doi.org/10.1074/jbc.M803953200

Warrant, E.J., and D.E. Nilsson. 1998. Absorption of white light in photoreceptors. *Vision Res.* 38:195–207. http://dx.doi.org/10.1016/S0042-6989(97)00151-X

Welsh, J.H., and C.M. Osborn. 1937. Diurnal changes in the retina of the catfish, *Ameiurus nebulosus*. *The Journal of Comparative Neurology.* 66:349–359. http://dx.doi.org/10.1002/cne.900660206

Wen, X.H., L. Shen, R.S. Brush, N. Michaud, M.R. Al-Ubaidi, V.V. Gurevich, H.E. Hamm, J. Lem, E. Dibenedetto, R.E. Anderson, and C.L. Makino. 2009. Overexpression of rhodopsin alters the structure and photoresponse of rod photoreceptors. *Biophys. J.* 96:939–950. http://dx.doi.org/10.1016/j.bpj.2008.10.016

West, R.W., and J.E. Dowling. 1975. Anatomical evidence for cone and rod-like receptors in the gray squirrel, ground squirrel, and prairie dog retinas. *J. Comp. Neurol.* 159:439–460. http://dx.doi.org/10.1002/cne.901590402

Westheimer, G. 1967. Dependence of the magnitude of the Stiles-Crawford effect on retinal location. *J. Physiol.* 192:309–315.

Winston, R. 1970. Light collection within the framework of geometrical optics. *Journal of the Optical Society of America.* 60:245–247. http://dx.doi.org/10.1364/JOSA.60.000245

Winston, R. 1981. The visual receptor as a light collector. *In* Vertebrate Photoreceptor Optics. Vol. 23. J.M. Enoch and F.L. Tobey Jr., editors. Springer-Verlag, New York. 325–336.

Wong, R.O.I. 1989. Morphology and distribution of neurons in the retina of the American garter snake *Thamnophis sirtalis*. *J. Comp. Neurol.* 283:587–601. http://dx.doi.org/10.1002/cne.902830412

Yacob, A., C. Wise, and Y.W. Kunz. 1977. The accessory outer segment of rods and cones in the retina of the guppy, *Poecilia reticulata* P. (Teleostei). An electron microscopical study. *Cell Tissue Res.* 177:181–193. http://dx.doi.org/10.1007/BF00221080

Young, H.M., and J.D. Pettigrew. 1991. Cone photoreceptors lacking oil droplets in the retina of the echidna, *Tachyglossus aculeatus* (Monotremata). *Vis. Neurosci.* 6:409–420. http://dx.doi.org/10.1017/S0952523800001279

Young, R.W. 1971. The renewal of rod and cone outer segments in the rhesus monkey. *J. Cell Biol.* 49:303–318. http://dx.doi.org/10.1083/jcb.49.2.303

Young, R.W. 1977. The daily rhythm of shedding and degradation of cone outer segment membranes in the lizard retina. *J. Ultrastruct. Res.* 61:172–185. http://dx.doi.org/10.1016/S0022-5320(77)80084-1

Young, S.R., and G.R. Martin. 1984. Optics of retinal oil droplets: a model of light collection and polarization detection in the avian retina. *Vision Res.* 24:129–137. http://dx.doi.org/10.1016/0042-6989(84)90098-1

Zaunreiter, M., H. Junger, and K. Kotrschal. 1991. Retinal morphology of cyprinid fishes: a quantitative histological study of ontogenetic changes and interspecific variation. *Vision Res.* 31:383–394. http://dx.doi.org/10.1016/0042-6989(91)90091-I

Zhang, X., T.G. Wensel, and C. Yuan. 2006. Tokay gecko photoreceptors achieve rod-like physiology with cone-like proteins. *Photochem. Photobiol.* 82:1452–1460.

Zyznar, E.S., and M.A. Ali. 1975. An interpretative study of the organization of the visual cells and tapetum lucidum of *Stizostedion*. *Canadian Journal of Zoology.* 53:180–196. http://dx.doi.org/10.1139/z75-023